DOI:10.14753/SE.2023.2813

POSTERIOR INTRALAMINAR COMPLEX OF THE THALAMUS AFFECTS SOCIAL INTERACTIONS

PhD thesis

Dávid Keller, MD

János Szentágothai Doctoral School of Neurosciences

Semmelweis University

Supervisor: Árpád Dobolyi, PhD, DSc

Official reviewers: Viktória Kormos, PhD

Balázs Hangya, PhD

Head of the Complex Examination Committee:

Alán Alpár, MD, PhD, DSc

Members of the Complex Examination Committee:

Kovács Krisztina, PhD, DSc

Tóth Zsuzsanna, PhD

Budapest, 2023

DOI:10.14753/SE.2023.2813

Table of Contents

DOI:10.14753/SE.2023.2813

List of Abbreviations

1. 3V – 3rd ventricle
2. ABC – Avidin-biotin-peroxidase complex
3. ac – Anterior commissure
4. ACSF – Artificial cerebrospinal fluid
5. ACN – Anterior commissural nucleus
6. APT – Anterior pretectal area
7. ASt – Amygdalostriatal transition area
8. Au1 – Primary auditory cortex
9. BLA – Basolateral amygdala
10. BMA – Basomedial amygdala
11. c-Fos-ir – C-Fos-immunoreactive
12. ca – Cerebral aqueduct
13. CB – Calbindin
14. CB-ir – Calbindin-immunoreactive
15. cc – Corpus callosum
16. CeA – Central amygdala
17. CG – Cingulate cortex
18. CGRP – Calcitonin gene-related peptide
19. CNO – Clozapine-N-oxide
20. cp – Cerebral peduncle
21. CPu – Caudate-putamen
22. CTB – Cholera toxin b subunit
23. Cu – Cuneate nucleus
24. Cx – Cerebral cortex
25. DLPAG – Dorsolateral periaqueductal grey
26. DMH – Dorsomedial hypothalamic nucleus
27. DMPAG – Dorsomedial periaqueductal grey
28. DMSO – Dimethyl sulfoxide
29. DR – Dorsal raphe nucleus
30. DREADD – Designer receptor exclusively activated by designer drug
31. DS – Dorsal subiculum

32. ec – External capsule
33. ECIC – External cortex of the inferior colliculus
34. f – Fornix
35. FITC – Fluorescein isothiocyanate
36. fmi – Forceps minor of the corpus callosum
37. Gr – Gracile nucleus
38. IC – Inferior colliculus
39. ILC – Infralimbic cortex
40. LaDA – Lateral amygdaloid nucleus, dorsal anterior part
41. LEnt – Lateral entorhinal cortex
42. LPAG – Lateral periaqueductal grey
43. LS – Lateral septal nucleus
44. LV – Lateral ventricle
45. MeA – Medial amygdaloid nucleus
46. MG – Medial geniculate body
47. MPL – Medial paralemniscal nucleus
48. MPA – Medial preoptic area
49. MPN – Medial preoptic nucleus
50. MPOA – Medial preoptic area
51. ml – Medial lemniscus
52. MS – Medial septal nucleus
53. mt – Mammillothalamic tract
54. Ni-DAB – Nickel-intensified 3,3-diaminobenzidine
55. ot – Optic tract
56. PAG – Periaqueductal central grey
57. PB – Phosphate buffer
58. PH – Posterior hypothalamic nucleus
59. PIL – Posterior intralaminar complex of the thalamus
60. Pit – Pituitary gland
61. PnO – Pontine reticular nucleus, oral part
62. PoT – Triangular subdivision of the posterior thalamic nucleus
63. PP – Peripeduncular nucleus

64. PTH – Parathyroid hormone
65. PTH1R – Parathyroid hormone receptor
66. PTH2 – Parathyroid hormone 2
67. PTH2-ir – Parathyroid hormone 2-immunoreactive
68. PTH2R – Parathyroid hormone 2 receptor
69. PTHrP – Parathyroid hormone related peptide
70. PV – Parvalbumin
71. PV-ir – Parvalbumin-immunoreactive
72. PVG – Periventricular grey of the thalamus
73. PVN – Paraventricular nucleus
74. py – Pyramidal tract
75. SC – Spinal cord
76. SN – Substantia nigra
77. SON – Supraoptic nucleus
78. Sp5 – Spinal trigeminal nucleus
79. TIP39 – Tuberoinfundibular peptide of 39 residues
80. TuLH – Tuberal region of lateral hypothalamus
81. V1 – Primary visual cortex
82. vBNST – Ventral bed nucleus of stria terminalis
83. vGATE – Virus-delivered Genetic Activity-induced Tagging of cell Ensembles
84. VLPAG – Ventrolateral periaqueductal grey
85. VMH – Ventromedial hypothalamic nucleus
86. VS – Ventral subiculum
87. ZI – Zona incerta

DOI:10.14753/SE.2023.2813

1. Introduction

1.1 The social behavior

1.1.1. The social behavior of animals

Social behavior can be defined as behavior affected by other members of the same species (1). It can be classified into different categories, including aggressive, mutualistic, cooperative, altruistic and parental (2). Different social behavior elements have different neuronal and endocrine background (1). Recent results indicate that two neural circuits are essential in forming the social behavior: the social behavior network and the mesolimbic reward system (3).

The social behavior network (SBN) includes all the neural components that regulate social behavior (4). The core nodes of the SBN take part in the regulation of several social behavior elements, they are connected to each other, and they often contain steroid hormone receptors. The SBN includes the following nodes: lateral septum, preoptic area, ventromedial hypothalamus, anterior hypothalamus, the periaqueductal gray, the medial amygdala, and the bed nucleus of the stria terminalis. All of these brain regions have been determined in mammals to participate in regulating reproductive and aggressive behaviors. The mesolimbic reward system is involved in the assessment of the relative importance and implications of an environmental stimulus, which evaluation is essential in forming a suitable behavioral response (3, 5, 6). A key element of this network is the dopaminergic innervation of the nucleus accumbens originating from the ventral tegmental area.

Rodents are the most used research subjects in many scientific fields. Due to the numerous social behavior studies, it is now also apparent how complex their social life is (7). It has also been demonstrated that rodents can acquire information on their environment through social transmission (8). They also use different modalities for social interactions, among them, the social touch is a major component. Although social touch is important in both sexual and nonsexual contexts in humans, too (9), in rodents, where modes of communication between conspecifics are more limited (note the lack of speech and limited mimicry) the role of social touch is relatively more important as part of the stereotypic behavioral repertoire for social interactions between individuals (10).

1.1.2. Role of hypothalamus and its oxytocin expressing neurons in the control of social behavior

The hypothalamus is a major regulatory center of rodent social behavior. It is also likely to be involved in the control of instinctive behaviors in humans (11). Social sensory inputs are known to reach the cerebral cortex via the thalamus, however, it is not known how information needed for social behavior arrives at the hypothalamus. Although, it is possible that information on social context reaches the hypothalamus via the cerebral cortex (12), it is also conceivable that ascending sensory pathways carrying information on social touch might project directly to the hypothalamus. Within the responsible neuronal circuits, neuropeptides have been implicated in the control of a variety of social behaviors.

Oxytocin, as a reproductive hormone, is secreted from the neurohypophysis to evoke uterus contraction and milk ejection in females during parturition and lactation, respectively (13). Oxytocin release within the central nervous system has recently gained major attention as a neuromodulator involved in promoting maternal behaviors (14-17) as well as social behaviors during non-lactating periods (18-21). In the rat brain, oxytocin-expressing neurons are located in the paraventricular (PVN) and the supraoptic (SON) nuclei (22). Magnocellular oxytocin neurons project to the pituitary and secrete oxytocin into the circulation (13, 23). Although, initially, only parvocellular oxytocin neurons were thought to project into brain and spinal cord regions, axon collaterals of magnocellular oxytocin neurons have recently been shown to also reach a number of brain areas (24). The targets of oxytocin neurons are often limbic areas involved in the social brain network (25, 26). Despite growing knowledge on the effects of oxytocin on social interactions (18, 19, 27), and the potential use of the oxytocin system as a drug target, e.g. in autism, eating and addictive disorders (28-30), surprisingly little information is available on the neuronal inputs leading to the activation of oxytocin neurons (31, 32). A combination of retrograde labeling and the c-fos technique identified inputs from the A1 and A2 noradrenergic cell groups as being important in conveying nociceptive and visceral information to the PVN (33, 34). These inputs have also been suggested to mediate reproductive influences (parturition, lactation) on oxytocin neurons (35, 36). Studies using electrophysiological and lesion techniques identified the mesencephalic lateral tegmentum, and more rostrally, the ventroposterior thalamic - peripeduncular area as parts of the milk ejection reflex arch

(37-42). However, the relay neurons in the milk ejection reflex pathway remained to be elucidated. Furthermore, it has not been established how information on social interactions reaches the oxytocin neurons (31).

1.2. The posterior intralaminar complex of the thalamus (PIL) and its neurons containing parathyroid hormone 2 (PTH2) neuropeptide

1.2.1. The PIL and its chemoarchitecture

The posterior intralaminar complex of the thalamus (PIL) is a triangular shape area in the thalamus, located ventromedial to the medical geniculate body and dorsal to the substantia nigra. The area can be easily distinguished from surrounding brain regions with the examination of the distribution of calcium binding proteins in and around the PIL (43). Parvalbumin (PV) immunolabeling was used to partially define the region. The ventral and the dorsomedial borders of the PIL can be identified by PV-immunoreactive (PV-ir) cell bodies in the substantia nigra and the anterior pretectal area, respectively (Fig. 1A). In contrast, the lateral and dorsal borders of the PIL made up of the peripeduncular area and the triangular subdivision of the posterior thalamic nucleus, cannot be differenciated using PV immunohistochemistry as they contain a low density of PV-ir cell bodies and fibers, as does the PIL (Fig. 1A). Parathyroid hormone 2 (PTH2) expressing neurons, which are evenly distributed within the PIL, differentiate it from the peripeduncular area and the triangular subdivision of the posterior thalamic nucleus that do not contain PTH2-immunoreactive (PTH2-ir) cell bodies.

The distribution of calbindin (CB) immunoreactivity is in sharp contrast to that of PV immunoreactivity in and around the PIL. The PIL contains a high density of calbindin-immunoreactive (CB-ir) cell bodies (Fig. 1B). Other brain regions adjacent to the PIL contain only very low density of CB-ir cell bodies. Within the PIL, both PTH2- and CB-ir cell bodies are evenly distributed. Furthermore, almost all PTH2-ir neurons contain CB immunoreactivity (Fig. 1C). CB-positive but PTH2-negative neurons are also present in the PIL and outnumber PTH2 neurons by about 2 times.

DOI:10.14753/SE.2023.2813

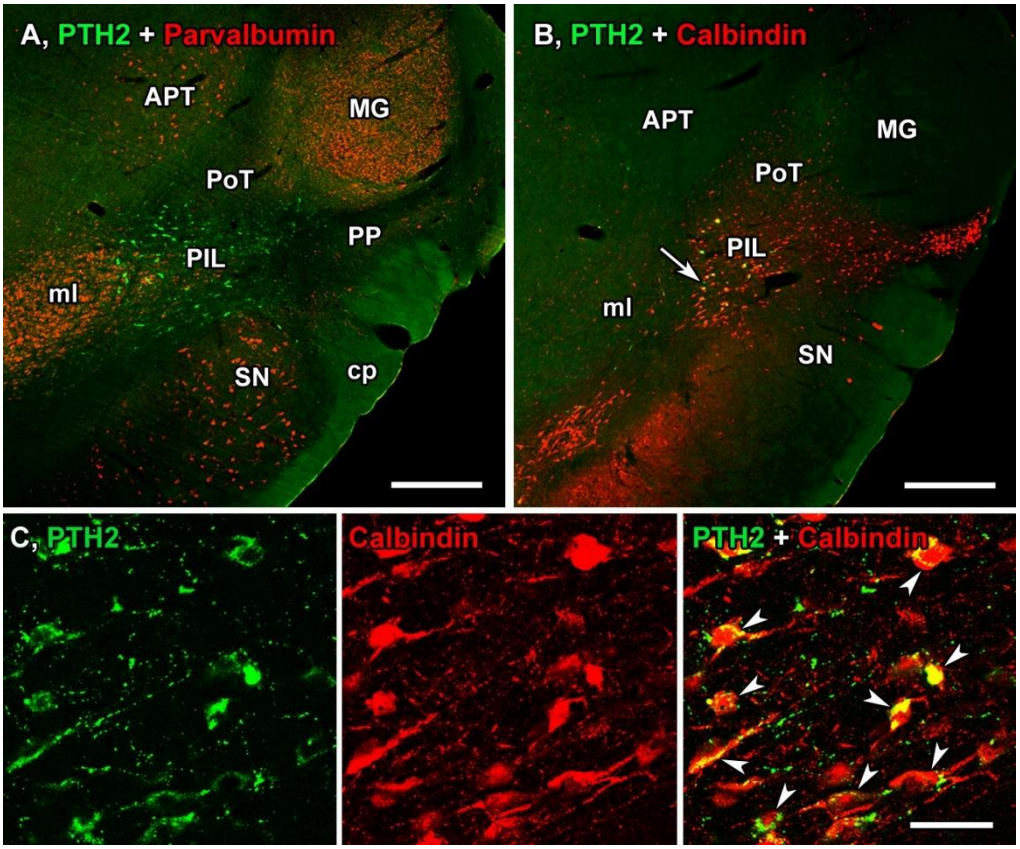

Figure 1. The chemical topography of the posterior intralaminar complex of the thalamus (PIL).

A, The localization of parvalbumin-ir neurons (red) in the area. Parvalbumin-ir neurons are abundant in the anterior pretectal area (APT) and in the substantia nigra (SN). In addition, a high density of parvalbumin-ir fiber terminals is present in the medial geniculate body (MG), while only a few labeled terminals are found in the PIL, the peripeduncular area (PP), and the triangular subdivision of the posterior thalamic nucleus (PoT). The distribution of PTH2 neurons (green) does not overlap with that of parvalbumin-ir neurons as PTH2 neurons are confined to the PIL. **B,** The localization of calbindin-ir (red) neurons in and around the PIL. Calbindin-ir neurons are present in the PIL and the PoT but are absent in the MG, APT, SN, and PP. The distribution of PTH2 neurons (green) overlap with that of calbindin-ir neurons in the PIL but not in the PoT. **C,** The fluorescent image of a section double labeled with calbindin (red) and PTH2 (green) corresponding to the indicated area in B shows that the majority of PTH2 neurons express calbindin (double labeling appears yellow). n=5. cp – cerebral peduncle, f – fornix. Scale bars: 750 μm for A and B and 100 μm for C. Source: (44).

1.2.2. The parathyroid hormone 2 (PTH2) neuropeptide

The parathyroid hormone 2 receptor (PTH2R) was discovered on the basis of its sequence similarity to other class B G-protein coupled receptors (45) and was named PTH2R because of its significant sequence similarity to the known parathyroid hormone receptor, which is now referred to as PTH1R; and because the human PTH2R is activated by parathyroid hormone (PTH) (46). Subsequently, an endogenous ligand of the receptor was identified following its purification from bovine hypothalamus. The new peptide was termed tuberoinfundibular peptide of 39 residues (TIP39) that time (47). The peptide is now categorized as parathyroid hormone 2 (PTH2). Despite its name, however, it is likely not a hormone as its presence in the blood has not been demonstrated. Rather, it is expressed mainly in the brain and has neuromodulatory functions. In addition, expression of PTH2 has been identified in some peripheral organs, such as the kidney, heart, and testis.

Rat (and mouse as these species have the same amino acid sequence for this gene) as well as human PTH2 (different in 4 amino acids) was demonstrated to be an agonist for the rat as well as the human PTH2R (47). It was shown to increase cAMP as well as intracellular Ca ion levels probably via Gs and Gq proteins, respectively (48, 49). While the known ligands for PTH1R, parathyroid hormone (PTH) and parathyroid hormone related peptide (PTHrP) have very few amino acid residues in common with PTH2, the only known endogenous ligand for PTH2R, their receptors, the PTH1R and PTH2R have about 50% amino acid identity when their sequences are aligned. Therefore, not surprisingly, the three peptides do have a similar three-dimensional structure (50). This motivated investigation of the relative receptor specificity of the ligands. PTH2 (either human or rat) does not activate the human or rat PTH1R. While PTH and PTHrP have similar potency at PTH1Rs, PTH (rat and human) but not PTHrP (human) activates the human PTH2R. Both rat and human PTH are, however, much less potent at the rat PTH2R. So while PTH does have some ability to activate the PTH2R, it is not likely that PTH is a natural ligand for PTH2R. PTH2R expression is greater in the brain than in peripheral tissues based on Northern blot, in situ hybridization histochemistry and immunohistochemistry (45, 47, 51), while the presence of PTH has not been demonstrated in the brain. Furthermore, in the rat, nanomolar concentrations of PTH do not cause significant activation of PTH2R (52). Nonetheless, the homologous structures

of the receptors and their peptide ligands facilitated experiments in which short sequences or residues were exchanged, allowing functional domains to be identified. Specifically, the amino terminus of the peptide ligand appears to be responsible for activation while the carboxyl region contributes much of the binding energy (53, 54). This information provided the basis for site-directed mutagenesis of PTH2 and the development of a high affinity antagonist of PTH2R by changing 4 residues of PTH2 and creating a peptide called HYWH-TIP39 (55).

1.2.3. PTH2 expressing neurons in the brain

Neuronal somas expressing PTH2 have been identified in just three brain sites in the adult rat and mouse brain based on the mapping of PTH2 mRNA expression and PTH2 immunopositive cell bodies (56), the periventricular grey of the thalamus (PVG), the posterior intralaminar complex of the thalamus (PIL), and the medial paralemniscal nucleus (MPL) in the lateral pons. Furthermore, no significant expression of PTH2 in other brain sites has been identified. However, the expression level changed in the three major expression sites during ontogeny. At embryonic day 16 during development, the expression of PTH2 was significant in the PIL but almost completely disappeared from this site during the first postnatal week. The PIL, an area ventromedial to the medial geniculate body, is a multisensory information processing relay station (57). In turn, the level of PTH2 increased in the PVG and MPL during postnatal development and started to decrease only around puberty (58). PTH2 expression levels also correlated with reproductive status as they were increased in the PIL and MPL of mother rats (59). PTH2-positive fibers have a much wider distribution, which includes limbic, autonomic, hypothalamic, nociceptive, and auditory brain regions (60). The distributions of PTH2-positive axon terminals and PTH2R display remarkable similarities, strengthening the argument that PTH2 is the endogenous ligand for PTH2R (61).

The distribution of the PTH2-PTH2R neuromodulator system is unique as it does not resemble that of any other system (56). In the PVG, PTH2 neurons are intermingled with the A11 dopaminergic neurons but do not display any co-localization. While A11 dopaminergic neurons have mostly descending projections (62), PTH2 neurons in this brain regions projects mostly towards the forebrain. Based on previous studies, this brain area may be involved in anti-nociception (63). In the PIL, PTH2 neurons have an

overlapping distribution with galanin-containing fibers, while neurons expressing calcitonin gene-related peptide (CGRP) are located immediately lateral to the PTH2 neurons. While the role of these CGRP neurons is not well known, they project towards the caudate-putamen and the perirhinal cortex (64). Projections of PIL neurons towards the amygdala were suggested to be involved in auditory fear conditioning (65). It has been suggested that the PIL can be divided into a medial and a lateral subdivision (66), the former expressing PTH2, the latter CGRP. The MPL is located immediately lateral to the A7 noradrenergic cell group and immediately medial to the intermediate nucleus of the lateral lemniscus. Because of the vicinity of this auditory relay nucleus, auditory functions of the MPL have been examined (67). The paralemniscal area could have a role in vocalization (68).

1.2.4. Behavioral effects of PTH2

The first indication of a potential effect of the PTH2-PTH2R system was the induction of PTH2 expression in the PIL (69) and MPL areas (70) around parturition and PTH2 levels remain elevated as long as the pups are present suggesting that suckling may activate PTH2 expression (59). Indeed, suckling induced c-Fos in PIL PTH2 neurons. In turn, if pups were returned to their mothers but a barrier between them prevented suckling, the activation of PIL PTH2 neurons was markedly reduced. Injection of an antagonist of PTH2 into the lateral cerebral ventricle (69), or locally into the arcuate nucleus via a lentivirus constitutively expressing and secreting the PTH2R antagonist HYWY-TIP39 in the locally infected cells decreased suckling-induced prolactin secretion (59). In line with these data, maternal absence of the PTH2R hindered postnatal pup development (71).

While prolactin is critically important for lactation and contributes to maternal behaviors (72), maternal behaviors are present even in the absence of prolactin suggesting independent routes for control of maternal behavior (73). Indeed, it was shown that neurons activated in mothers by pups include those which are not sensitive to prolactin (74). The preoptic area of the hypothalamus is the area most critical for maternal behaviors in rodents (75). Since PTH2 fibers and PTH2R are abundant in this brain region (76), the effect of PTH2 on maternal behaviors was addressed. Local administration of PTH2R antagonist into the preoptic area, performed by the PTH2R antagonist HYWY-

TIP39 expressing lentivirus described above, reduced pup-induced place preference, suggesting a role of PTH2 in maternal attachment and motivation (69). A possible target of PTH2 is galanin-containing preoptic neurons as these cells, known to govern some aspect of maternal behaviors including retrieving of the pups to the nest (77), are innervated by PTH2 fibers (78). Additional cell types in the preoptic area also participate in the control of maternal behaviors (79, 80), which may also contribute to the mediation of PTH2 action.

PTH2 was recently demonstrated to sense the presence of conspecifics in zebrafish via mechanoreceptors in the lateral line organ (81). The level of PTH2 increased after the social exposure in previously isolated fish and decreased after isolation is socially reared fish. They also demonstrated that the sensory modality that controls the expression of PTH2 was not visual in origin but was mechanical, induced by the movements of neighboring fish.

Since out of the potential thalamic PTH2-expressing cell groups, the PTH2-expression was only induced in the PIL, not in the PVG, therefore we hypothesize that the PIL gives neuronal input to the oxytocin secreting cells and has a potential role in the control of social behavior.

DOI:10.14753/SE.2023.2813

2. Objectives

A, Investigation of the connection of the PIL with the social brain network

1. Description of the efferent projections of the PIL using adeno-associated viral tract tracing.

2. Injection of cholera toxin b subunit (CTB) retrograde tracer into the PIL to reveal the sources of information that activate these neurons. CTB-immunoreactive cells are examined in the spinal cord, as well as in lower and higher brain regions.

B, Functional evidence of the role of the PIL in the control of social behavior

1. Assessment the c-Fos activation in the PIL following social interaction of females, in comparison with isolated control animals. Neurochemical identification of the c-Fos activated neurons is also addressed.

2. Demonstration of the functional evidence of the role of the PIL in social interactions by means of stimulation and inhibition of its neurons using viral gene transfer and chemogenetics. Freely moving social behavior test, as well as social interaction test without direct contact. Test of locomotion is also performed as behavioral control.

3. Examination of the effect of chemogenetic-based manipulation of PIL neurons tagged by previous social contact experience. A Tet-Om system is used to express stimulatory and inhibitory receptors into c-Fos activated neurons.

C, Role of the PTH2-expressing neurons of the PIL during social interactions

1. To establish the activation of PTH2 in the control of social behavior, the expression level of PTH2 mRNA in the PIL neurons is compared between animals kept in social environment or chronically isolated using quantitative real-time PCR.

2. The role of PTH2 in social interactions is addressed in experiments investigating the effect of antagonizing PTH2 receptor on the social behavior of female rats. For that purpose, a PTH2 receptor antagonist is injected into the lateral ventricle using osmotic minipumps.

3. To address where PTH2 may exert its actions on social behavior, we describe the distribution of PTH2 fibers in relation to the social neuropeptide oxytocin.

4. The origin of PTH2 fibers in the PVN is determined by injection of the retrograde tracer CTB into the PVN. The type of retrogradely labeled PIL neurons is also evaluated.

3. Methods

Animals

The Workplace Animal Welfare Committee of the National Scientific Ethical Committee on Animal Experimentation at Semmelweis and Eötvös Loránd Universities, Budapest, specifically approved this study (PE/EA/926-7/2021 and PE/EA/568-7/2020, respectively). A total of 125 adult female rats (Wistar; Charles Rivers Laboratories, Hungary) were used.

Histology

Animal brain tissue collection and sectioning

Rats were deeply anesthetized and perfused transcardially. Serial coronal sections were cut, on which immunolabeling was performed. The injection sites of viruses as well as the projection pattern of the infected neurons was studied using immunoperoxidase technique with the visualization of mCherry, for which a chicken anti-mCherry antiserum (1:1,000; Abcam) was used with Ni-DAB method. For fiber density analysis of PIL projections, we used the machine learning based pixel classification feature of the free bioimage analysis software QuPath v0.2.3 (Queen's University Belfast and University of Edinburg) (82). Double labeling of PTH2 with calbindin or parvalbumin was carried out using an affinity-purified anti-PTH2 antiserum (1:3,000) validated previously (83, 84). Then, mouse anti-calbindin D-28k (1:1,500; Sigma) or mouse anti-parvalbumin antiserum (1:2,500; Sigma) was applied at room temperature overnight.

Tracer experiments

Cholera toxin b subunit (CTB) injections

The retrograde tracer CTB was targeted to the PVN (n = 10), and to the PIL (n = 15) in lactating mother rats at postpartum day 4. The relation of the injection site to the position of PTH2 immunoreactivity was verified by double labeling. Some of the misplaced injections were used as controls. For stereotaxic injections, rats were positioned in a stereotaxic apparatus with the incisor bar set at -3.3 mm 4 days after delivery. Holes of about 2-mm diameter were drilled into the skull above the target coordinates. Glass micropipettes of 15–20-μm internal diameter were filled with 0.25% CTB dissolved in PB. The CTB was injected by iontophoresis by using a constant current source that

delivered a current of +6 μA, which pulsed for 7 sec on and 7 sec off for 15 min. Then the pipette was left in place for 10 min with no current and withdrawn under negative current. After tracer injections, the animals were allowed to survive for 7 days.

Double immunolabeling of CTB and PTH2 or calbindin

Every fourth free-floating section was first stained for PTH2 by using FITC-tyramide amplification fluorescent immunocytochemistry (n=5). Sections were then incubated overnight in goat anti-CTB (1:10,000) or mouse anti-calbindin antisera followed by Alexa594 anti-goat and anti-mouse IgG for 1 h.

Social c-Fos activation study

Social interaction experiment

Female rat littermates (n=8) kept together (housed 2 per cage) were used in the study. The two rats were isolated for 22 h to reduce basal c-Fos activation. Then, the rats were reunited again in the cage they had cohabited (n=4). Control females (n=4) continued to be kept isolated. All animals were sacrificed 24 h after the beginning of isolation, i.e. 2 h after reunion of the socially interacting group. Animals were perfused transcardially as described above, and processed for c-Fos immunohistochemistry.

c-Fos immunohistochemistry

The procedure was performed for immunolabeling using rabbit anti-c-Fos primary antiserum (1:3000; Santa Cruz Biotechnology) and Ni-DAB visualization.

Double immunolabeling of c-Fos and calbindin

Sections were placed in rabbit anti-c-Fos primary antiserum (1:20000) for 24 h at room temperature. Subsequently, sections were treated with FITC-tyramide (1:8000) and H_2O_2 in Tris hydrochloride buffer for 6 min. Then, the mouse anti-calbindin D-28k antiserum was applied at room temperature overnight.

Analysis of c-Fos immunolabeling

The sections containing the greatest number of c-Fos immunoreactive (c-Fos-ir) neurons in the PIL was selected from each of the 8 animals, and an image was taken of them using 10x objective. The total number of c-Fos-ir neurons in the selected brain area was counted using ImageJ 1.53e program (NIH, Bethesda, MD). Statistical analyses were performed using Prism 9 for Windows (GraphPad Software, Inc., La Jolla, CA). The number of c-Fos-ir neurons was compared using two-tailed unpaired t-test.

Viral vector-based chemogenetics

Chemogenetic activation or silencing of the PIL

rAAV-**P**$_{hSYN}$-hM3D(Gq)-mCherry (n=7); rAAV-**P**$_{hSYN}$-hM4D(Gi)-mCherry (n=10) or rAAV-**P**$_{hSYN}$-mCherry (n=8) was injected to the PIL. Some of the misplaced injections were used as controls in tract tracing. For stereotaxic injections, rats were positioned in a stereotaxic apparatus with the incisor bar set at -3.3 mm. Holes of about 1 mm diameter were drilled into the skull above the target coordinates. A Hamilton pipette (volume 1 µl) was filled with the solution containing the virus and lowered to the following stereotaxic coordinates: AP = −5.2 mm from bregma, ML = ±2.6 mm from the midline, DV = −6.8 mm from the surface of the dura mater. Once the pipette was in place, 100 nl virus was pressure injected into the PIL (10 nl/min), then the pipette was left in place for 10 min. Following the slow withdrawal of the pipette, we repeated the same protocol on the other side of the brain. After the injections, the animals were isolated for two weeks for recovery, then they were reunited with their familiar cagemate for one week before the behavior tests took place.

Activity-dependent tagging: Chemogenetic manipulation of PIL neurons activated upon social encounter

The protocol for bilateral injections of the vGATE viral cocktail into the PIL was as described above. The viral cocktail included the following viruses: 1. rAAV-(tetO)$_7$-**P**$_{fos}$-rtTA; 2. rAAV-**P**$_{tet}$bi-Cre/YC3.60; 3. rAAV-**P**$_{hSYN}$-DIO-hM3D(Gq)-mCherry (n=9) or rAAV-**P**$_{hSYN}$-DIO-hM4D(Gi)-mCherry (n=8) or rAAV-**P**$_{hSYN}$-DIO-mCherry (n=6). 600 nl of single injection contained the following: 1st virus: 225 nl. 2nd virus: 75 nl, 3rd virus: 300 nl (3/1/4 ratio). After two weeks of recovery, the animals were treated with i.p. doxycycline hyclate injection (5 mg/kg bw dissolved in the mixture of 0.01M PBS and 0.9% NaCl, 2 : 1 ratio), then, the following day, they were reunited with one of their cagemates for 2 hours for expression of DREADD in neurons that are c-Fos-positive in the PIL in response to social interaction.

Osmotic minipump

For the direct and sustained infusion of PTH2R antagonist, HYWH-TIP39 into the lateral ventricle, we used Alzet® Osmotic Minipump, Durect™ (0.5 µl/h, 14 days, 0.3 ml)

combined with Alzet® Brain Infusion Kit 2, Durect™ with two spacers attached. Cannula was inserted into the LV (V = 4.0 mm) and fixed to the skull with cranioplastic cement. The osmotic minipump was placed at the back of the animal subcutaneously and was filled with artificial cerebrospinal fluid (ACSF, n=7) or PTH2 receptor antagonist (n=6).

Social behavioral tests

Clozapine-N-oxide (CNO) injection

In case of the viral vector-based chemogenetics, 1.5 h before the behavioral experiments, the animals were isolated from their cagemates, which was followed by the intraperitoneal administration of CNO or vehicle. On the first day of the experimental session, we used control vehicle injection (5% dimethyl sulfoxide (DMSO) dissolved in distilled water, 1 ml/kg bw). One day later, CNO was administered i.p. (0.3 mg/kg bw CNO, dissolved in 5% DMSO dissolved in distilled water, 1 ml/kg bw). This was followed by another control injection three days later.

Freely moving social behavior test

The animals were habituated to the open field arena (40 x 80 cm) one day before the experiment. On the experimental day, the animals were placed in the open field arena where the subject and the stimulus rat could freely interact with each other and 10 minutes of footage was recorded. The following social behavior elements were distinguished (7, 21) (Fig. 1A): anogenital sniffing (“one individual sniffs or licks the anogenital region of a conspecific”), non-anogenital sniffing (“one individual shows enhanced sniffing at colony members”), chasing (“one individual runs after a second”), social grooming (“one individual gently nibbles or licks the fur of a conspecific, sometimes with the aid of its forepaws”, mounting (“walks over a conspecific, that is typically the more dominant”, and passive social interaction (one gets into contact with conspecific without performing one of the above mentioned behavior elements, e. g. side-to-side contact).

The duration of the different types of performed behaviors were measured by using Solomon Coder software (https://solomon.andraspeter.com/). The duration of the behavioral elements was compared between the groups using repeated measures ANOVA followed by Šídák's multiple comparisons tests.

Social interaction test without direct contact

In another experiment, direct contact between the animals was not allowed. Instead, the stimulus rat was placed in a small cage with wall made of bars, so they could just smell, hear and see each other while 10 min of footage was recorded (Fig. 1B).

The behavior of the animals in the experiment excluding the physical contact was analyzed with SMART Video Tracking software v3.0 (Panlab Harvard Apparatus). The duration of social interaction without direct contact (when the experimental rat approached the small cage within 5 cm) was compared between the groups using one-way ANOVA followed by Šídák's multiple comparisons tests.

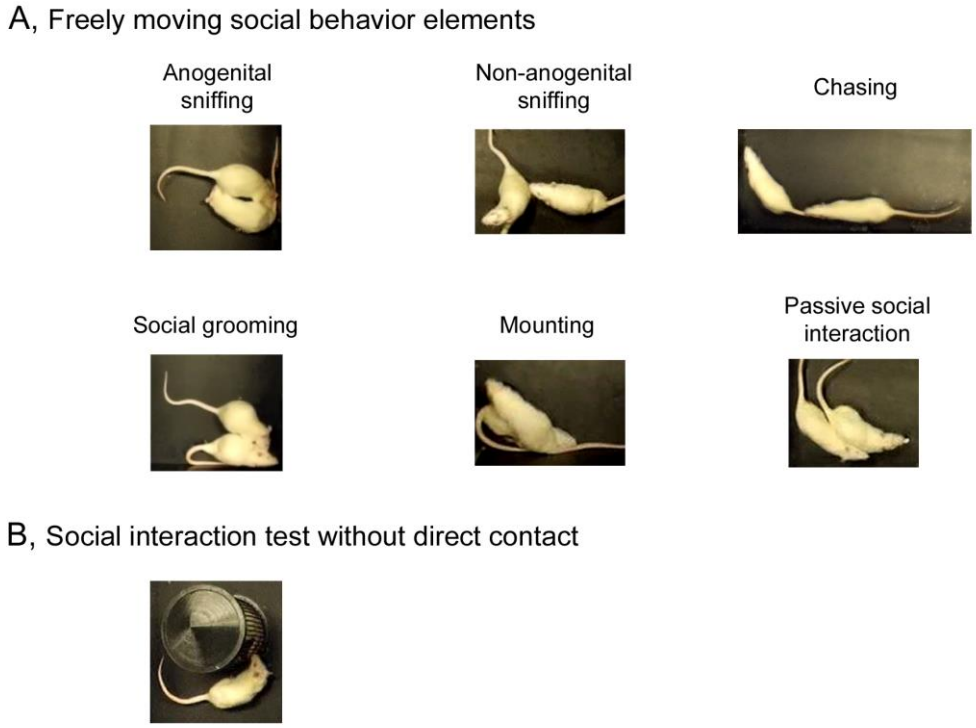

Figure 2. Distinguished social behavior elements of the rats.

A, Behavior elements of the animals in the freely moving social behavior test: anogenital sniffing, non-anogenital sniffing, chasing, social grooming, mounting and passive social interaction. **B,** Demonstration of the social interaction test without direct contact. Source: (44).

Microdissection of brain tissue samples and Real-time PCR

For qRT-PCR, brains were dissected from 10 female adult rats kept in social environment (3 animals/cage) and 10 female adults isolated for two weeks prior to dissection. Immediately after the dissections of the brain, the PIL was microdissected as described

previously in mother rats (69). The dissected tissue samples were quickly frozen in Eppendorf tubes on dry ice, and stored at -80°C until further processing.

Real-time qRT-PCR was carried out as described previously (85). Total RNA was isolated from frozen PIL tissue samples using TRIzol reagent (Invitrogen, Carlsbad, CA, USA) as lysis buffer combined with RNeasy Mini kit (Qiagen, Germany) following the manufacturer's instructions. The PCR reactions were performed with iTaq DNA polymerase in total volumes of 12.5 µl under the following conditions: 95°C for 3 min, followed by 35 cycles of 95°C for 0.5 min, 60°C for 0.5 min, and 72°C for 1 min. The data were expressed as the ratio of the housekeeping gene GAPDH using the following formula: log(Ct(GAPDH)-Ct(PTH2)). Statistical analyses were performed by unpaired t-test for comparisons of the two groups.

Microscopy and image processing

Sections were examined using an Olympus BX60 light microscope equipped with fluorescent epi-illumination. Confocal images were acquired with a Zeiss LSM 780 confocal Microscope System using 40-63 X objectives at an optical thickness of 1 µm for counting varicosities and 3 µm for counting labeled cell bodies. For demonstration purposes, contrast and sharpness of the images were adjusted using the "levels" and "sharpness" commands in Adobe Photoshop CS 9.0.

Statistics

All statistical calculations were carried out using GraphPad Prism (GraphPad Software, LLC, released 2020, version 9.0.0.). Data were first tested with Shapiro-Wilk test for normality. If the data were normally distributed, we used two-tailed paired t-test for two groups which were related to each other. When the comparison was made between two different groups, we used two-tailed unpaired t-test (e. g. qRT-PCR study or social c-Fos study). Otherwise, if the data came from a non-normal distribution, we performed Wilcoxon matched-pairs signed rank test (for comparing two groups) or Friedman test followed by Dunn's multiple comparisons tests (for comparing more groups). In case of the comparison between more normally distributed groups repeated measures ANOVA (freely moving social behavior test) were performed followed by Šídák's multiple comparisons tests.

DOI:10.14753/SE.2023.2813

4. Results

4.1. Efferent projections of the PIL

To determine neuronal connections of PIL neurons, rAAV-**P**$_{hSYN}$-hM3D(Gq)-mCherry virus was injected into the PIL of female rats (Fig. 3 A). The infected cells withdrew the virus and it was transported anterogradely. Labeled axons were found in a number of socially-relevant brain regions, such as the infralimbic cortex (ILC), lateral septum (LS), medial preoptic area (MPOA; including the medial preoptic nucleus (MPN) and the medial preoptic area (MPA)), ventral bed nucleus of stria terminalis (vBNST), paraventricular hypothalamic nucleus (PVN), amygdala (A), dorsomedial hypothalamic nucleus (DMH) and periaqueductal central grey (PAG) (Fig. 3A).

Following control injections of the virus into the adjacent substantia nigra the labeled fibers were present only in the caudate-putamen, and not in the target areas of the PIL (Fig. 3B).

DOI:10.14753/SE.2023.2813

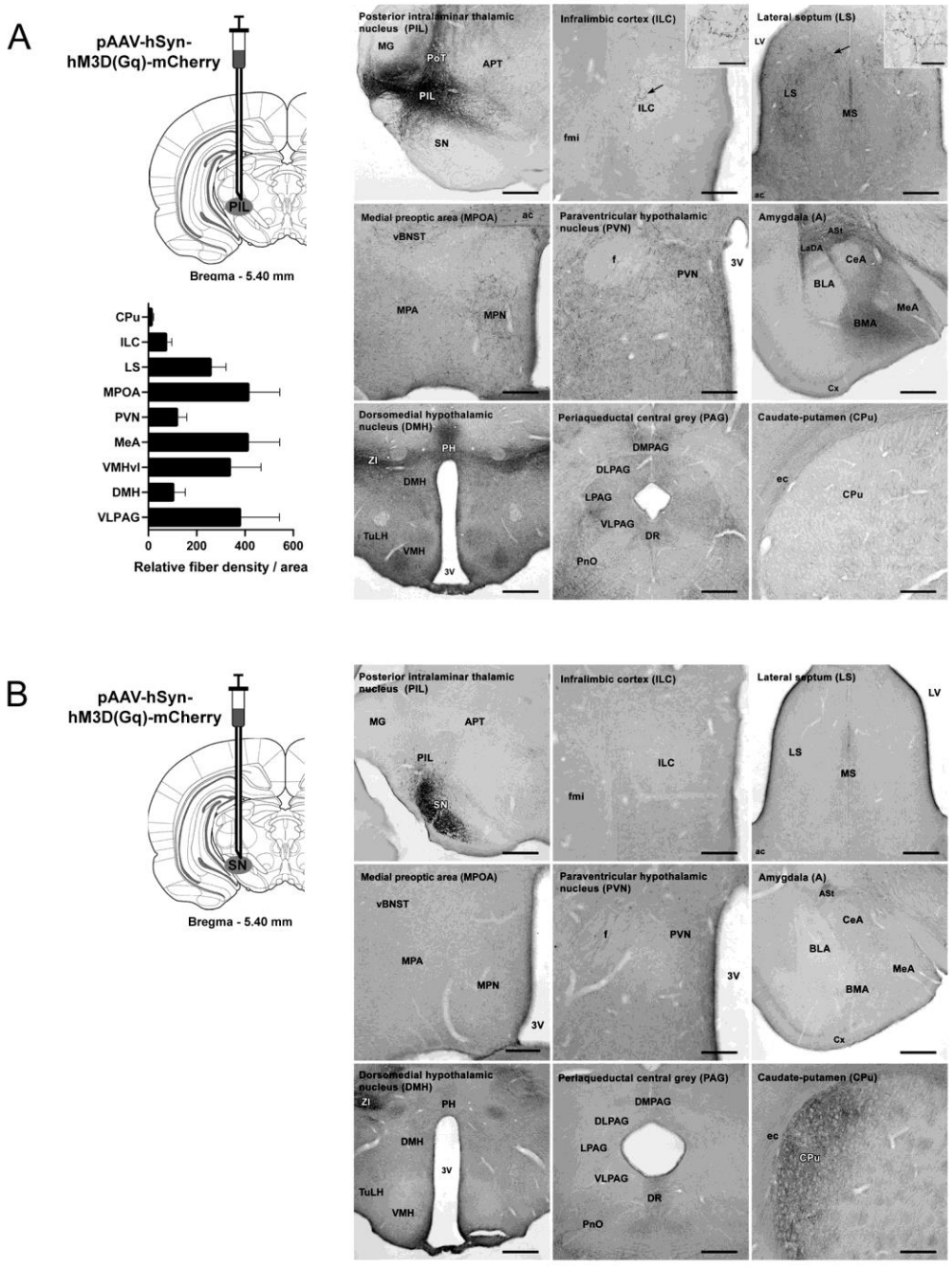

Figure 3. The anterograde spread of the virus injected into the PIL or SN to socially implicated brain regions.

A, The virus (rAAV-$\mathbf{P}_{hSYN}$-hM3D(Gq)-mCherry) was injected into the PIL followed by mCherry immunolabeling to visualize virus-containing cells and fibers. Density of the mCherry-positive fibers = mCherry immunolabeled area / total area of the annotation * 10^4, n=8. Values are mean ± s.e.m. Scale bars: 300 μm for ILC and PVN, 375 μm for MPOA, 525 μm for CPu, 600 μm for LS, 750 μm for PIL, A, DMH and PAG and 30 μm

for the insets. **B,** The control injection site included the SN, but not the PIL (n=3). In contrast to the injection into the PIL, no fibers were found in the socially implicated brain regions, but there were abundant terminals in the CPu. Scale bars: 300 μm for ILC and PVN, 375 μm for MPOA, 525 μm for CPu, 600 μm for LS and 750 μm for PIL, A, DMH and PAG. Source: (44).

4.2. Afferent projections of the PIL

We also investigated the afferent connections of the PIL. We injected the retrograde tracer cholera toxin b subunit (CTB) into the PIL to identify the neurons that project to it and used injections into adjacent regions for comparison (Fig. 4A–D). Injections that did not overlap the PIL, including into varying parts and amounts of the substantia nigra, triangular subdivision of the posterior thalamic nucleus, medial lemniscus, and peripeduncular nucleus resulted in labeling patterns markedly different from those following PIL injections and generally lacked labeling in areas that were labeled by PIL injections. The majority of cells projecting to the PIL were ipsilateral to the injection side except for the gracile and cuneate nuclei and the spinal cord, where there was contralateral dominance.

Inputs from lower brain regions and the spinal cord

The spinal cord contained CTB labeled neurons contralateral to the injection site. These neurons were distributed in Rexed laminae IV-VII throughout the thoracic and lumbar segments that were sectioned. The cells were typically located in laminae IV-V in thoracic segments (Fig. 4E) and laminae VI-VII in lumbar segments (Fig. 4F). We rarely found more than one labeled cell in a coronal section; on average, every 4th coronal spinal cord section contained a labeled cell. The labeled cells usually had oval perikarya with multiple dendrites (Fig. 4 E and F).

In the medulla oblongata, the gracile and cuneate nuclei had the highest density of CTB-containing cells (Fig. 4G). The spinal trigeminal nucleus, particularly the deep layers of its ventral portion, also contained a significant number of labeled cells (Fig. 4G). In these nuclei, the CTB-labeled neurons were located contralateral to the injection site. Only a few regions in the upper brainstem contained any CTB-positive neurons. The highest number of labeled cells was in the external cortex of the inferior colliculus (Fig.

4H) while the lateral parabrachial nucleus, the periaqueductal gray and the deep layers of the superior colliculus contained a low number.

Inputs from higher brain regions

Within the cerebral cortex, the auditory areas contained a considerable number of retrogradely labeled neurons. The insular cortex and the medial prefrontal cortex contained a few CTB-positive neurons, with the highest density of labeled cells in the infralimbic cortex. Other cortical areas were devoid of CTB signal. Retrograde labeling was also absent from most other forebrain structures. We only detected a significant number of labeled neurons in the central amygdaloid nucleus, the substantia innominata, and the anterior portion of the lateral septal nucleus. Within the diencephalon, the largest number of labeled cells was within the ventromedial hypothalamic nucleus, particularly in its ventrolateral subdivision (Fig. 4I). A considerable number of CTB neurons were also located in the lateral preoptic area, and the zona incerta.

DOI:10.14753/SE.2023.2813

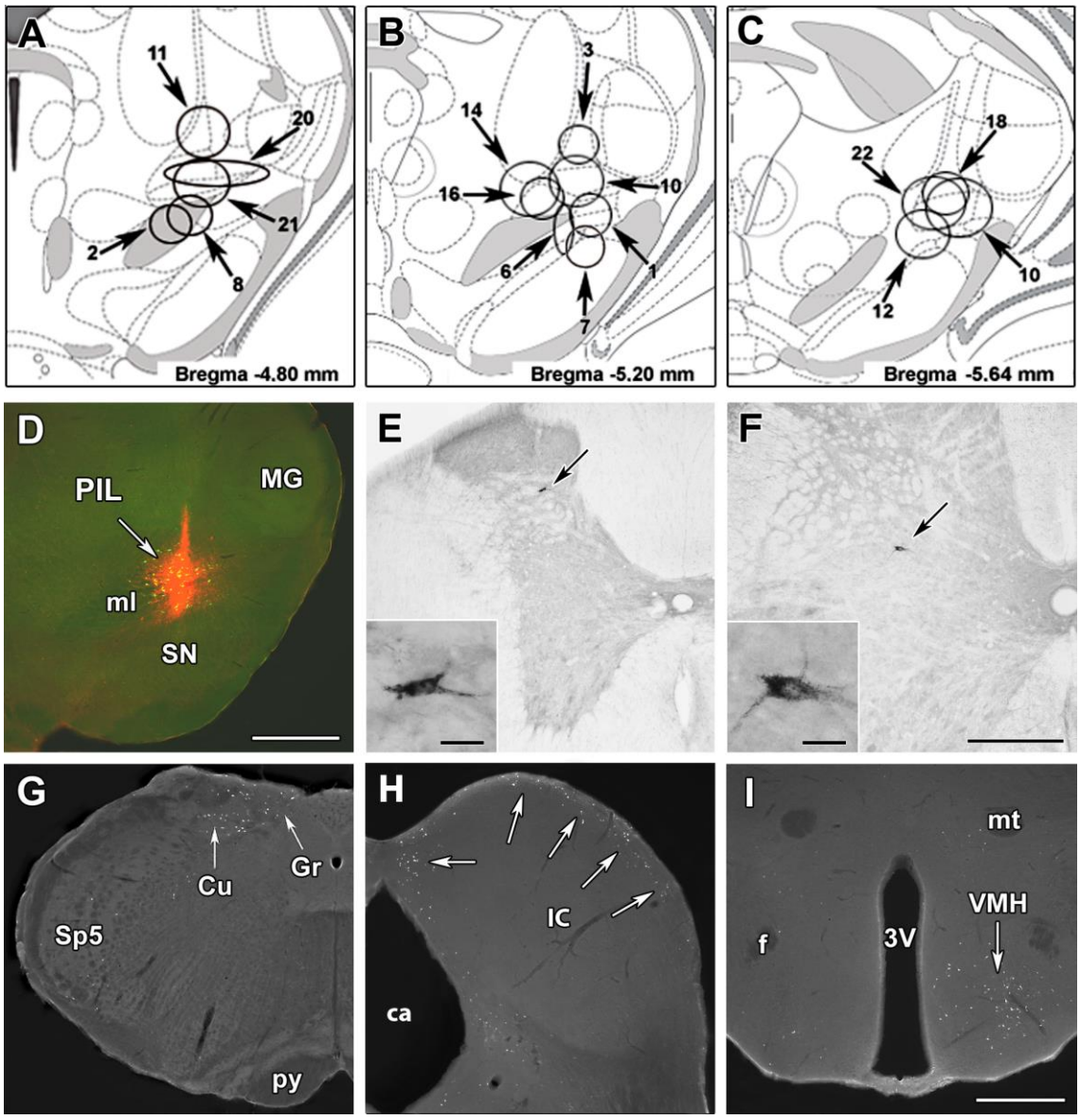

Figure 4. The afferent neuronal connections of the posterior intralaminar complex of the thalamus (PIL).

A-C, The sites where the retrograde tracer cholera toxin beta subunit (CTB) spread in the coronal plane following injections in particular animals are circled. Drawings were prepared by aligning the pictures adapted from a rat brain atlas (86). The three drawings represent coronal sections at bregma levels -4.80 mm, -5.20 mm, and -5.64 mm. The injection sites are shown at the level closest to the center of the injection. **D,** The injection site belonging to animal No. 10 is shown double labeled with PTH2 to show that CTB injection site (red) overlaps with the location of PTH2 neurons (green; yellow in combination with red) in the PIL. **E-I,** CTB-labeled cell bodies are shown in the spinal cord at the level of thoracic segment 2 (E) and lumbar segment 5 (F) as well as in different

brain regions including the gracile (Gr) and cuneate nuclei (Cu) in the medulla oblongata (G), the external cortex of the inferior colliculus (H), and the ventromedial hypothalamic nucleus (VMH), especially its ventrolateral subdivision (I). n=15. 3V – 3rd ventricle, ca – cerebral aqueduct, f – fornix, MG – medial geniculate body, ml – medial lemniscus, mt – mammillothalamic tract, py – pyramidal tract, SN – substantia nigra, Sp5 – spinal trigeminal nucleus. Scale bars: 1 mm for D, G, H and I, 400 μm for E and F, and 30 μm for insets. Source: (43).

4.3. Activation of the PIL neurons in response to social interaction between female rats

As the next step, we examined the c-Fos activation of PIL neurons following social interactions. Female littermates grown up together were separated for 22 h to reduce basal c-Fos activity. When females were reunited for 2 h after the 22 h separation, they engaged in social interactions. For about a combined 1 h, the animals had direct body contact, of which they slept next to each other for 20 min. These behaviors were associated with a significantly elevated number of c-Fos immunoreactive (c-Fos-ir) neurons in the PIL (Fig. 5A) as compared to rats that were kept isolated (Fig. 5B). C-Fos-ir neurons appeared evenly distributed within the PIL. Their distribution corresponded with that of the calbindin-ir neurons (Fig. 5C). In fact, the majority (86%) of the c-Fos-ir neurons contained calbindin (Fig. 5D). The number of Fos-ir neurons in the PIL section with the largest number of labeled cells was 169 ± 14 after social interaction with a familiar female while there were only 41 ± 8 in the isolated group, which represents a highly significant increase ($p < 0.001$). The activation of cells in the PIL was specific as adjacent structures, such as the medial geniculate body and the substantia nigra, did not show an increase in the number of c-Fos-ir neurons. In fact, an elevated number of c-Fos-ir neurons were observed in only a relatively small number of brain regions including the medial prefrontal cortex, medial preoptic area, and amygdala.

DOI:10.14753/SE.2023.2813

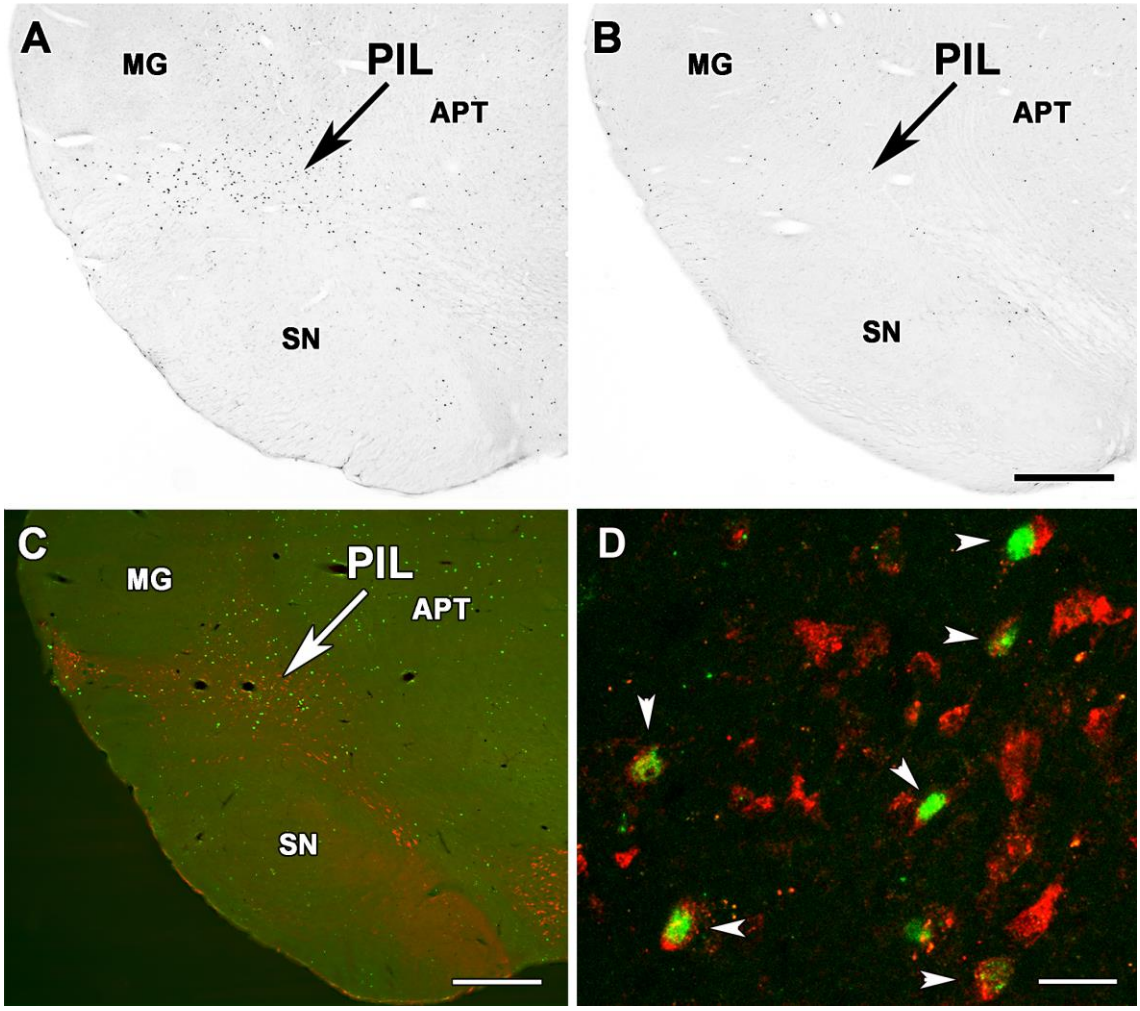

Figure 5. C-Fos immunoreactivity in the PIL in response to social interactions.

A, C-Fos activation in neurons of familiar female rats in familiar environment. C-Fos-ir neurons (black dots) are abundant in the PIL 2 h after reuniting rats that were housed together and then separated for 22 h. The adjacent medial geniculate body (MG) and substantia nigra (SN) are almost completely devoid of c-Fos activation while a lower density of labeled cells are visible in the anterior pretectal nucleus (APT). **B,** In animals not reunited with each other, only a few c-Fos labeled neurons are present in the PIL. **C,** The distribution of c-Fos-ir neurons (green) completely overlaps with that of the calbindin-ir neurons (red) in the PIL upon social interactions. **D,** A high magnification confocal image demonstrates that the majority of c-Fos-ir neurons contain calbindin immunoreactivity, indicated by white arrowheads. n=4 for each group. Scale bar: 500 μm for A, B and C, 30 μm for D. Source: (43).

4.4. Behavioral effects of chemogenetically manipulated PIL neurons

To investigate whether PIL manipulation affects social behaviors, we injected excitatory (recombinant adeno-associated virus (rAAV)-**P**$_{hSYN}$-hM3D(Gq)-mCherry), inhibitory (pAAV-**P**$_{hSYN}$-hM4D(Gi)-mCherry) designer receptor exclusively activated by designer drug (DREADD) expressing or control viruses (rAAV-**P**$_{hSYN}$-mCherry) into the PIL of female rats. The rats, in which over 80% of the virally infected cells were only included in the behavioral analysis. The animals were subsequently housed individually for two weeks, and then reunited for 1 week (Fig. 6A) prior to injection of clozapine-N-oxide (CNO), the agonist of the DREADD. Almost all (90.4 ± 3.4%) activated cells contained mCherry and almost all (88.9 ± 3.0%) mCherry-positive neurons in the PIL showed c-Fos-positivity 1.5 hours after CNO administration, which validates the effectiveness of our chemogenetic stimulation (Fig. 6 B and C).

Next, we investigated several distinct social behavioral elements during a 10 min following activation or inhibition of PIL neurons. Duration of social grooming significantly increased upon the chemogenetic stimulation as compared to previous day but also as compared to vehicle injection on the following day (Fig. 6D). Data from individual animals are shown for social grooming. In turn, inhibition of the PIL neurons reduced grooming as compared to the control days (Fig. 6E). In the absence of a DREADD, the viral infection and the CNO administration did not affect social grooming (Fig. 6F). Note that the stimulation and the inhibition of PIL neurons has the opposite effect of social grooming while other behavioral elements were not affected by the manipulation or changed the same direction by the different treatments (non-anogenital sniffing).

We also performed an experiment in which direct contact between the animals was prevented by separating them by a bar wall which still allowed them to smell, hear and see each other. Chemogenetic activation of the PIL had no effect on the duration of social interaction under these conditions, highlighting the importance of direct contact as the effect of induced activation of the PIL (Fig. 6G).

DOI:10.14753/SE.2023.2813

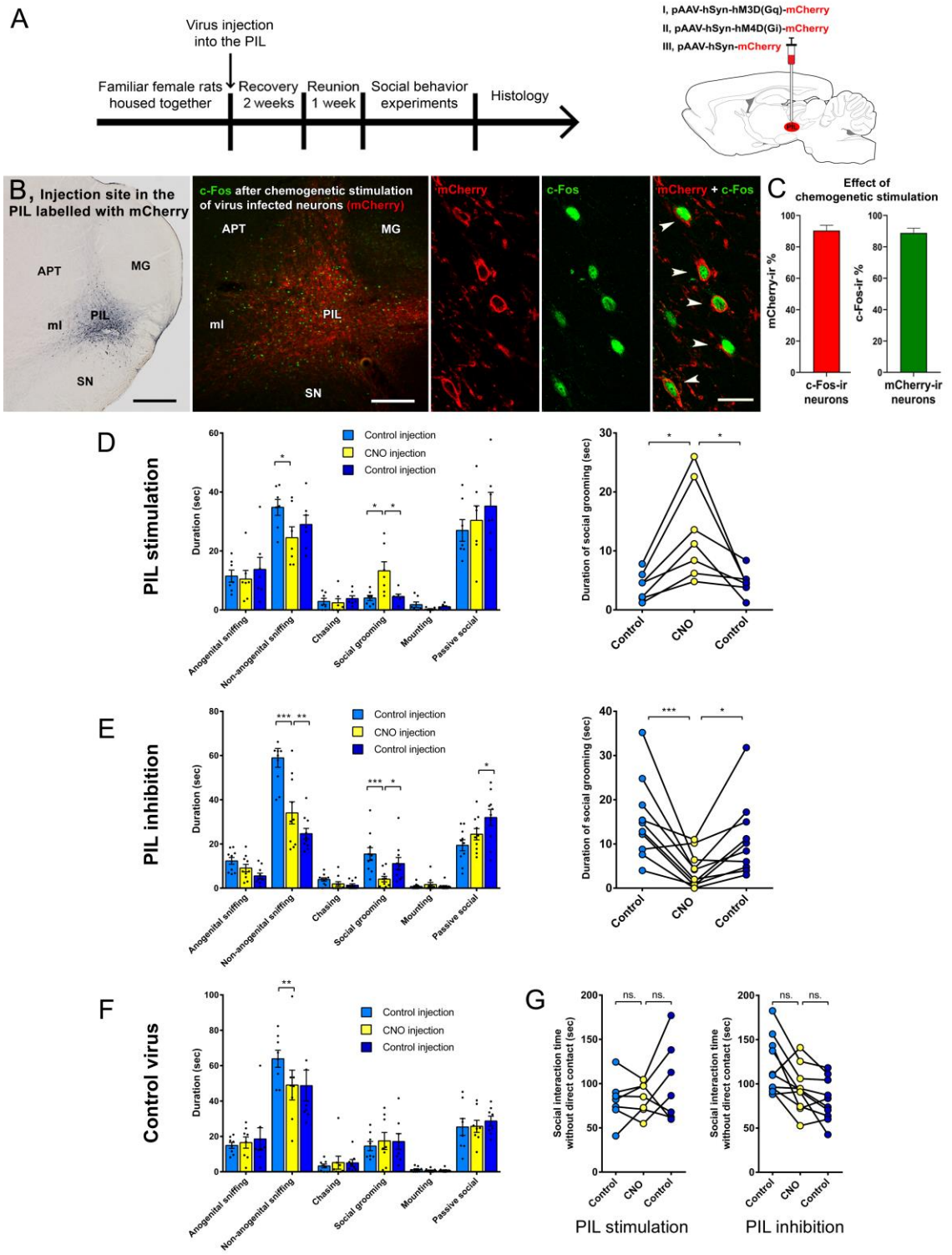

Figure 6. Effect of chemogenetic manipulation of PIL on social grooming in female rats.

A, Experimental protocol of the chemogenetic manipulation of the PIL in female rats. **B,** The PIL as the injection site of the virus expressing mCherry fluorescent tag, and the *in vivo* validation of the effectiveness of chemogenetic stimulation. The PIL is located in

the posterior part of thalamus in rat, dorsal from the substantia nigra (SN) and ventromedial from the medial geniculate body (MG). DREADD-expressing mCherry-immunopositive neurons (red) colocalized with c-Fos (green) in response to CNO injection. APT – anterior pretectal area, ml – medial lemniscus. Scale bars: 750 μm (left), 300 μm (middle) and 60 μm (right). **C,** Quantification of CNO-induced c-Fos expression in the PIL. Most of the c-Fos expressing cells were mCherry-positive while most of the mCherry-positive neurons were activated after the injection of CNO, n=6. **D,** Chemogenetic stimulation of PIL neurons in freely moving adult females. n=7, repeated measures ANOVA followed by Šídák's multiple comparisons tests, for social grooming: $p = 0.028$ (1^{st} control *vs.* CNO) and $p = 0.041$ (CNO *vs* 2^{nd} control). **E,** Chemogenetic inhibition of PIL neurons in freely moving adult females. n=10, repeated measures ANOVA followed by Šídák's multiple comparisons tests, for social grooming: $p = 0.0005$ (1^{st} control *vs* CNO) and $p = 0.0495$ (CNO *vs* 2^{nd} control). **F,** The absence of effect of control virus on the social interaction in freely moving adult females. n=8, repeated measures ANOVA followed by Šídák's multiple comparisons tests, for social grooming: $p = 0.88$ (1^{st} control *vs* CNO) and $p = 0.99$ (CNO *vs* 2^{nd} control). **G,** Chemogenetic stimulation and inhibition of PIL in absence of physical contact. For stimulation n=7, one-way ANOVA followed by Šídák's multiple comparisons tests, $p = 0.99$ (1^{st} control *vs* CNO) and $p = 0.64$ (CNO *vs* 2^{nd} control); for inhibition n=10, one-way ANOVA followed by Šídák's multiple comparisons tests, $p = 0.072$ (1^{st} control *vs* CNO) and $p = 0.14$ (CNO *vs* 2^{nd} control). $0.010 < *p < 0.050$, $0.001 < **p < 0.010$ and $***p < 0.001$. Values are mean ± s.e.m. Source: (44).

4.5. Chemogenetic investigation of socially tagged PIL neurons

To selectively manipulate PIL neurons activated by previous social exposure, we used the **v**irus-delivered **G**enetic **A**ctivity-induced **T**agging of cell **E**nsembles (vGATE) method (87). Excitatory, inhibitory and control viral cocktails (rAAV-$(tetO)_7$-$\mathbf{P}_{fos}$-rtTA; rAAV-$\mathbf{P}_{tet}$bi-Cre/YC3.60; rAAV-$\mathbf{P}_{hSYN}$-DIO-hM3D(Gq)-mCherry/ rAAV-$\mathbf{P}_{hSYN}$-DIO-hM4D(Gi)-mCherry/pAAV-$\mathbf{P}_{hSYN}$-DIO-mCherry) were injected into the PIL of female rats. In the vGATE system, a c-fos promoter ($\mathbf{P}_{fos}$) fragment drives the expression of the reverse tetracycline sensitive (tet) transactivator (rtTA). Following the recovery of the animals, a single intraperitoneal doxycycline administration launched the autoregulatory

expression loop of $(tetO)_7$-rtTA, thus opening the labeling period. The following day, the subjects were reunited with a cagemate in their home cage for 2 hours as direct social exposure, which resulted in the expression of the DREADD or control sequence in social contact experienced vGATE-tagged neurons only (encoded in the third virus: rAAV-**P**$_{hSYN}$-DIO-hM3D(Gq)-mCherry, rAAV-**P**$_{hSYN}$-DIO-hM4D(Gi)-mCherry or rAAV-**P**$_{hSYN}$-DIO-mCherry) (Fig. 7A). Social behavior experiments were conducted 10 days later and then the brains were processed for histological analysis.

Labeling of calcium-binding proteins revealed that the PIL region infected with the vGATE viruses was surrounded by parvalbumin-positive cells, and that the vast majority of the calbindin-positive cells were vGATE labeled (90.6%; n =3). To validate the applied vGATE method, we performed c-Fos immunolabeling after direct social exposure or isolation (Fig. 7B). 2.4-times more cells were labeled for c-Fos after social exposure (32.2 ± 4.0; n = 3) than after isolation (13.4 ± 4.3; n = 2), which is a significant difference (two-tailed unpaired t-test, $p = 0.011$). 54.0% ± 5.5% of the mCherry cells were double labeled with c-Fos after social interaction compared with 21.5% ± 6.7% after isolation (two-tailed unpaired t-test, $p = 0.0044$; Fig. 7C).

During the direct contact social behavior test, where the animals could freely interact with each other, the duration of social grooming significantly increased following the stimulation of PIL vGATE-tagged neurons (Fig. 7D), and in turn, the duration of social grooming significantly decreased following the inhibition of PIL vGATE-tagged neurons (Fig. 7F). Furthermore, no behavioral changes were found in the group injected with the control virus (Fig. 7H). Notably, only direct physical contact elicited an increase in social interactions time after chemogenetic manipulation of vGATE-tagged PIL neurons (Fig. 7 E, G and I).

We also performed an open-field test with the CNO injected animals to measure their locomotor activity. The total distance covered by the animals was not affected by driving the activity of PIL neurons suggesting that the altered social behaviors were not a consequence of altered locomotor drive.

Social behaviors initiated by the experimental and opponent animals were separately examined. Manipulation of socially tagged PIL neurons by the injection of CNO changed the behavior initiated by experimental animals. In contrast, the social interactions initiated by the other animal were not affected.

DOI:10.14753/SE.2023.2813

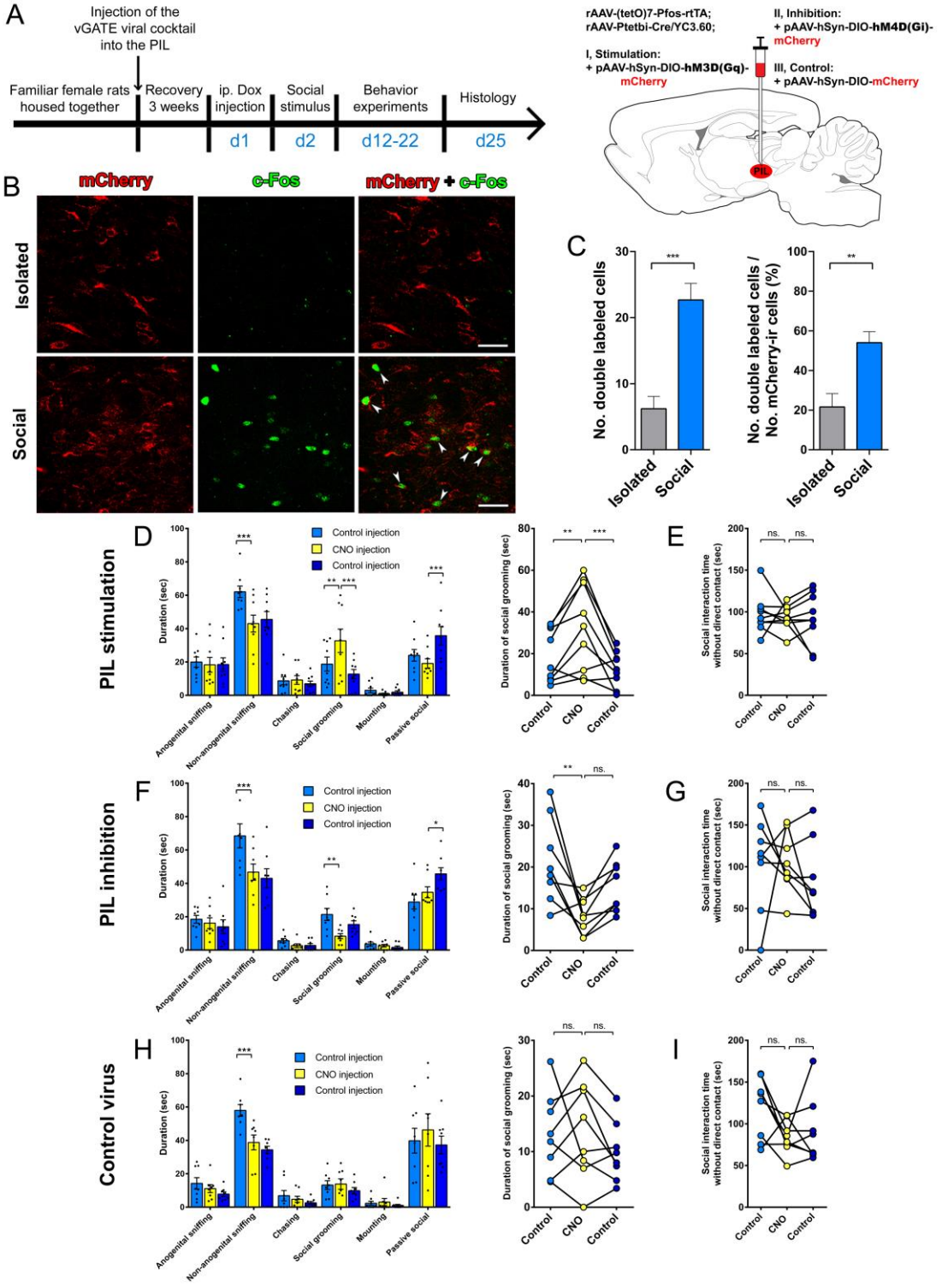

Figure 7. Effects of the manipulation of PIL using vGATE viral cocktail.

A, Experimental protocol of the chemogenetic PIL manipulation using vGATE viruses. **B,** *In vivo* validation of the vGATE technique: neurons infected by the vGATE viruses were activated after social exposure (indicated by white arrowheads) but not in isolated control animals. Scale bars: 75 μm. **C,** Quantification of social-induced c-Fos expression

in the vGATE-tagged PIL. Significantly more cells were labeled for c-Fos after social exposure than after isolation. In addition, significantly more mCherry cells were double labeled with c-Fos after social interaction compared with the number of cells labeled after isolation. n=3 for social, n=2 for isolation. **D,** vGATE stimulation of PIL neurons in freely moving adult females. n=9, repeated measures ANOVA followed by Šídák's multiple comparisons tests, for social grooming: $p = 0.0019$ (1st control *vs* CNO) and $p < 0.001$ (CNO *vs* 2nd control). **E,** vGATE stimulation of PIL in absence of physical contact. n=9, one-way ANOVA followed by Šídák's multiple comparisons tests, $p = 0.96$ (1st control *vs* CNO) and $p = 0.99$ (CNO *vs* 2nd control). **F,** vGATE inhibition of PIL neurons in freely moving adult females. n=8, repeated measures ANOVA followed by Šídák's multiple comparisons tests, for social grooming: $p = 0.0018$ (1st control *vs* CNO) and $p = 0.16$ (CNO *vs* 2nd control). **G,** vGATE inhibition of PIL in absence of physical contact. n=8, one-way ANOVA followed by Šídák's multiple comparisons tests, $p > 0.99$ (1st control *vs* CNO) and $p = 0.46$ (CNO *vs* 2nd control). **H,** The effect of vGATE control virus on the social interaction in freely moving adult females. n=8, repeated measures ANOVA followed by Šídák's multiple comparisons tests, for social grooming: $p = 0.99$ (1st control *vs* CNO) and $p = 0.69$ (CNO *vs* 2nd control). **I,** The effect of vGATE control virus on the social interaction in absence of physical contact. n=8, one-way ANOVA followed by Šídák's multiple comparisons tests, $p = 0.14$ (1st control *vs* CNO) and $p = 0.95$ (CNO *vs* 2nd control). $0.010 < *p < 0.050$, $0.001 < **p < 0.010$ and $***p < 0.001$. Values are mean ± s.e.m. Source: (44).

4.6. Role of PTH2-expressing PIL neurons in the control of social behavior

Our further aim was to investigate the role of PTH2 in the control of social behavior. Following the microdissection of PIL, we compared the expression of PTH2 mRNA using quantitative real-time PCR (Fig. 8A). We found that the expression of PIL PTH2 mRNA was 2.4-times higher in animals kept in a social environment (together with conspecifics in their home cage) compared to control animals socially isolated for two weeks (Fig. 8B).

We also performed an experiment infusing PTH2R antagonist into the lateral ventricle of female rats via osmotic minipumps (Fig. 8C). The results demonstrate an important role of PTH2 in the control of social grooming because this behavioral element

was specifically reduced in the experimental group of the animals, which received the PTH2R antagonist, compared with the artificial cerebrospinal fluid (ACSF) infused control group (Fig. 8D).

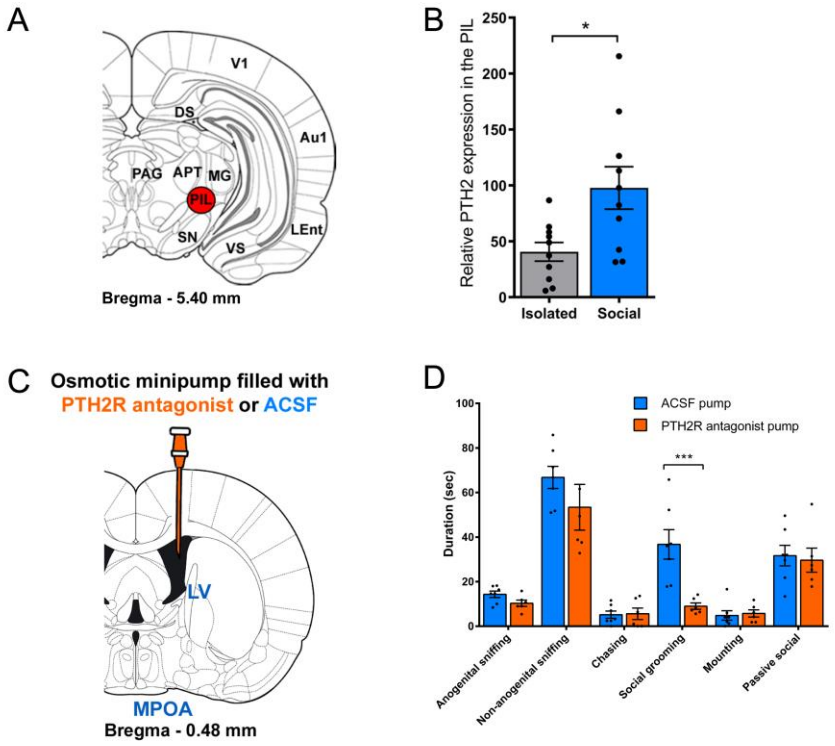

Figure 8. The role of PTH2 in the control of social behavior.

A, The PIL is located in the posterior part of thalamus in rat, dorsal from the SN and ventromedial from the MG as shown in a drawing of the rat brain (86). The marked area (red) was dissected for mRNA measurement. **B,** Significantly higher PTH2 expression was found in the PIL in animals kept in a social environment as compared to isolated controls, using quantitative RT-PCR. mRNA level of PTH2 / mRNA level of housekeeping gene * 10^6, n=10 (each group), two-tailed unpaired t-test, *p = 0.013. Values are mean ± s.e.m. **C,** Experimental design of infusion of an antagonist of the PTH2 receptor into the lateral ventricle of female rats using osmotic minipumps. **D,** The effect of the PTH2 receptor antagonist on the social behavior of freely moving animals. n=7 for artificial cerebrospinal fluid (ACSF) and n=6 for PTH2R antagonist, repeated measures ANOVA followed by Šídák's multiple comparisons tests, for social grooming: $p < 0.001$. ***$p < 0.001$. Values are mean ± s.e.m. Source: (44).

4.7. Close apposition of oxytocin neurons by PTH2-containing axon terminals

Within the anterior hypothalamus, the PVN (Fig. 9A), its anterior subdivision, the anterior commissural nucleus (ACN), and the SON receive a dense innervation by PTH2 containing fibers. In these nuclei, the distribution of PTH2 fibers overlapped with the distribution of oxytocin neurons (Fig. 9B and E). We also found that the majority of oxytocin neurons were closely apposed by PTH2-containing varicosities (Fig. 9 C, D and F). The average number of close apposition on the soma and proxymal dendrites of oxytocin neurons was 2.28 ± 0.38 in the parvocellular paraventricular, 1.90 ± 0.39 in magnocellular paraventricular, and 0.42 ± 0.20 in supraoptic oxytocin neurons. We did not observe a clustering of the oxytocin neurons that were closely apposed by PTH2-containing varicosities in either the PVN or the SON.

DOI:10.14753/SE.2023.2813

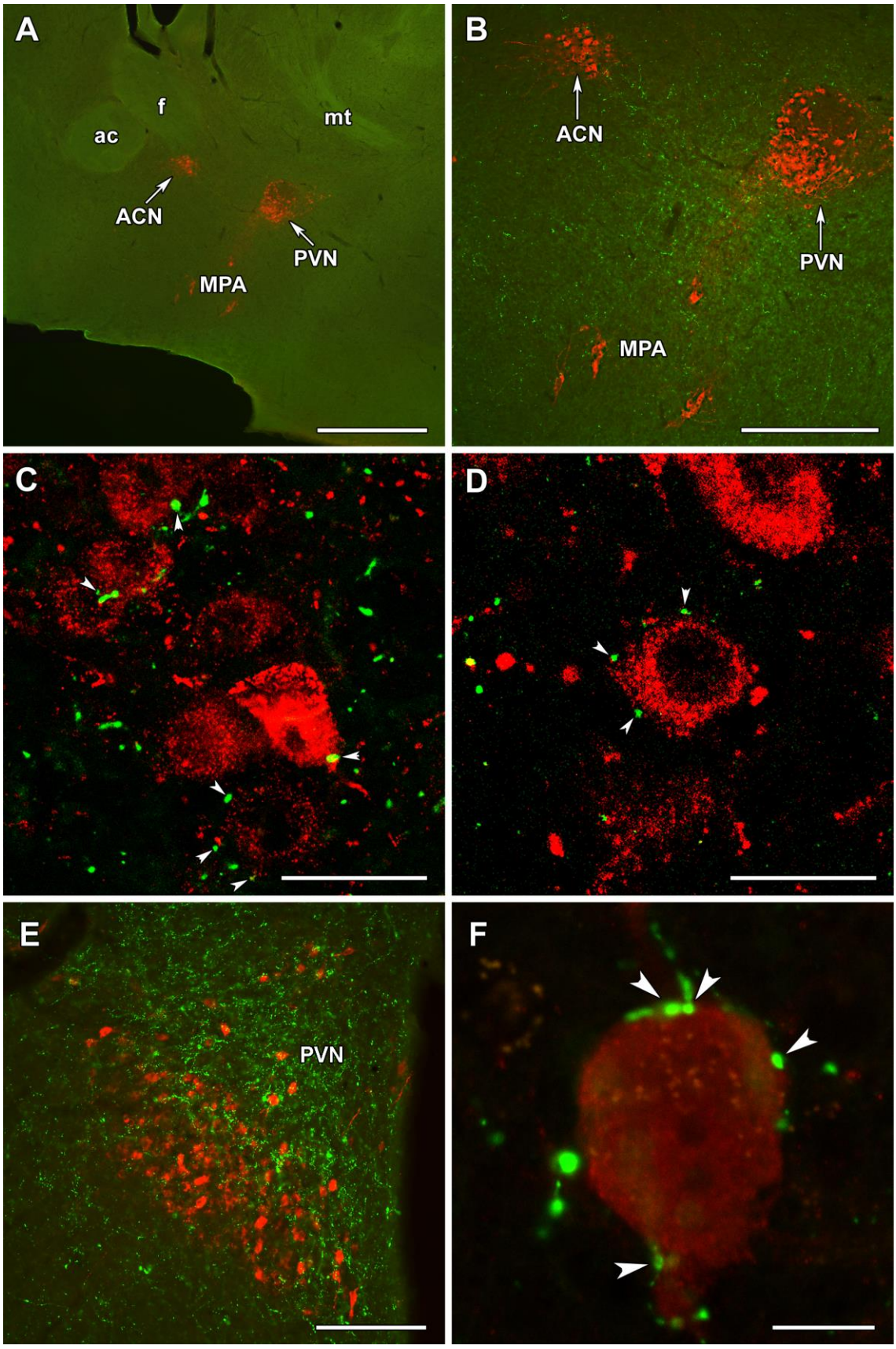

Figure 9. Close apposition of oxytocin neurons in the hypothalamus by fiber terminals containing PTH2.

A, A sagittal section of the hypothalamus reveals that oxytocin neurons (red) are present in the paraventricular (PVN) and a major accessory nucleus, the anterior commissural (ACN) nucleus, as well as other accessory cell groups in the medial preoptic area (MPA). **B,** There are abundant PTH2-positive nerve fibers (green) in these regions. **C-D,** At the sagittal section of the hypothalamus, PTH2-containing nerve fiber terminals closely appose the cells bodies of the oxytocin-positive neurons (indicated by white arrowheads) in the ACN (C) and the PVN (D). **E,** Coronal section of the PVN demonstrates that PTH2-ir terminals (green) in the PVN overlap with the location of oxytocin-ir neurons (red). **F,** The high magnification confocal image demonstrated that PTH2-ir varicosities closely appose cell bodies and proximal dendrites of oxytocin-ir cell bodies at the coronal section of the PVN. The white arrowheads point to close appositions. n=6. ac – anterior commissure, f – fornix, mt – mammillothalamic tract. Scale bars: 1 mm for A, 500 μm for B, 50 μm for C, 30 for μm D, 200 μm for E and 20 μm for F. Sources: (43, 88).

4.8. Retrograde labeling in the PIL following tracer injections into the PVN

To identify the source of its PTH2 innervation we injected the retrograde tracer CTB into the PVN. There were 4 injections with a large overlap between the area of tracer deposition and the territory occupied by PTH2 fibers within the PVN, animals 3, 5, 8, and 9 in Fig. 10. The pattern of retrogradely labeled cells was similar for these injections including a particularly high number of CTB-immunoreactive (CTB-ir) neurons in the ipsilateral lateral septum, the bed nucleus of the stria terminalis, several hypothalamic regions, the supramammillary nucleus, some thalamic regions, and the parabrachial nuclei. In addition, all these injections resulted in a large number of labeled neurons in the PIL. There was a predominantly ipsilateral labeling of cells that were distributed uniformly throughout the PIL but there were no labeled cells in adjacent brain regions (Fig. 10C). Double-labeling showed that 45% of the CTB labeled neurons in the PIL contained PTH2 immunoreactivity. In turn, the PVN-projecting PIL neurons contained calbindin (Fig. 10D). When the injection site overlapped only partially with the PVN (animals 4, 6, and 10), only few CTB-ir cells in the PIL while CTB-labeled cells were not

DOI:10.14753/SE.2023.2813

present in the PIL in animals 1, 2, and 7 whose injection site did not overlap with the PVN.

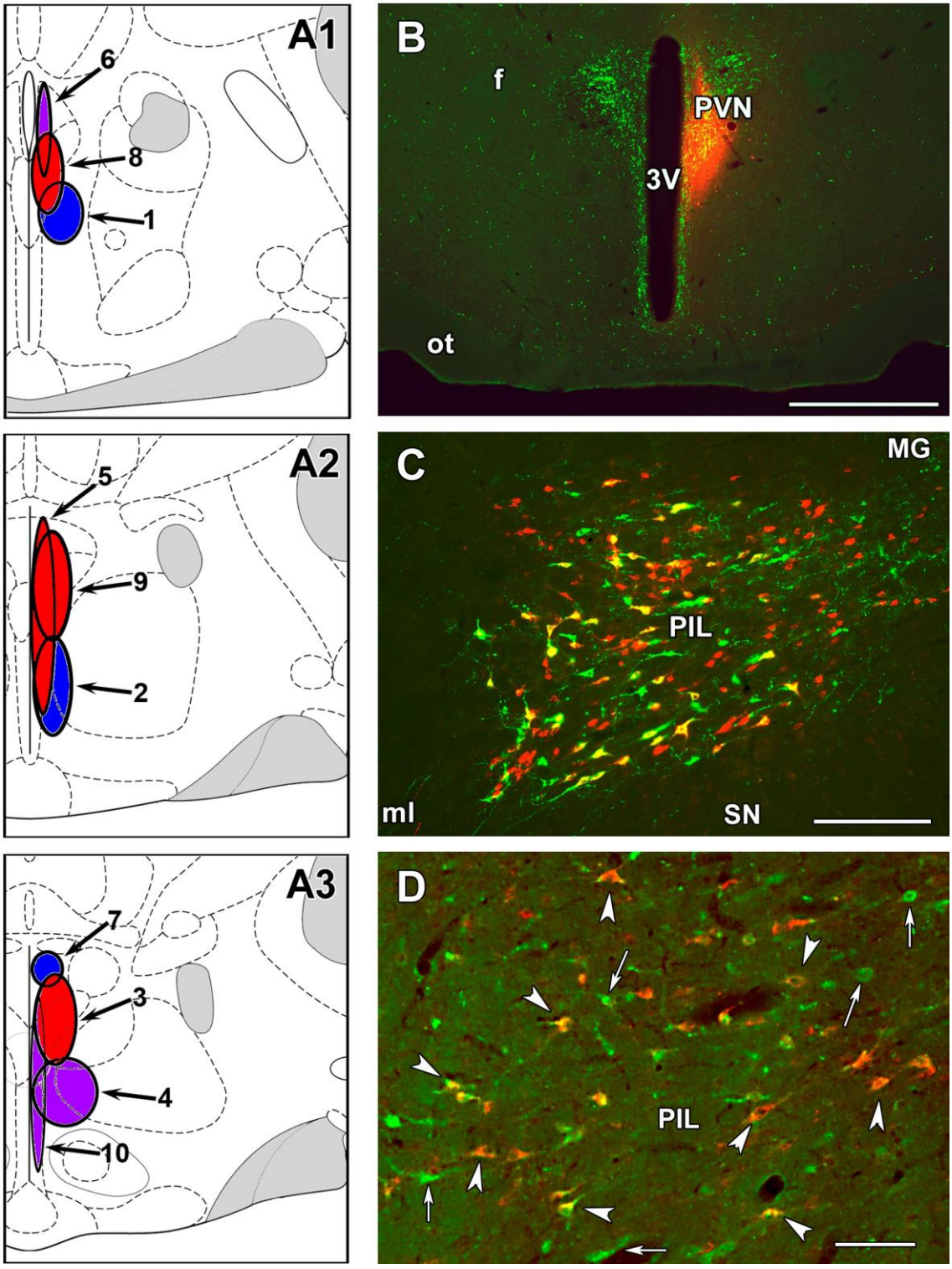

Figure 10. Projection of the PIL to the PVN.

A, The sites where the retrograde tracer CTB spread in the coronal plane following injections in particular animals are circled. Drawings were prepared by aligning the pictures with corresponding schematics adapted from a rat brain atlas (86). The three drawings represent coronal sections at bregma levels -1.2 mm (A1), -1.6 mm (A2), and -1.8 mm (A3). The injection sites are shown at the level closest to the center of the injection. The numbers connected to the injection sites by arrows represent the number of the particular animal in the experiment. Injection sites with red, purple, and blue colors represent many, few, and no retrogradely labeled cells in the PIL, respectively. **B,** The injection site of rat #9 is shown for demonstration purposes. The spread of CTB (red) overlaps with a great portion of PTH2-ir fibers (green) located in the PVN. **C,** A high number of retrogradely labeled CTB-ir neurons (red) are visible among the PTH2-ir (green) neurons in the ipsilateral PIL. A high percentage of the retrogradely labeled neurons are double labeled as indicated by the yellow color. **D,** Essentially all CTB-ir neurons (red) are labeled with calbindin (green), as well. Some examples are shown by white arrowheads. Single labeled calbindin-ir neurons are also visible (white arrows). n=10. 3V – 3rd ventricle, f – fornix, MG – medial geniculate body, ml – medial lemniscus, mt – mammillothalamic tract, ot – optic tract, PIL – posterior intralaminar complex of the thalamus, SN – substantia nigra. Scale bars: 1 mm for B and 300 μm for C, and 100 μm for D. Source: (43).

5. Discussion

5.1. The posterior intralaminar complex of the thalamus (PIL) and its afferent and efferent neuronal connections

The PIL, defined by the area containing PTH2 neurons in mother rats, includes the posterior intralaminar thalamic nucleus and also the parvicellular subparafascicular nucleus and some parts of the caudal subdivision of the zona incerta (89). In this brain area, calbindin-ir neurons are confined to the PIL except for the triangular subdivision of the posterior thalamic nucleus dorsally adjacent to the PIL, which contains calbindin-ir neurons, but not PTH2 neurons. The distribution of calbindin immunoreactivity in this study was the same as reported previously in the area but called the parvocellular part of the subparafascicular nucleus (90). The PIL also corresponds to the posterior intralaminar complex described as containing calbindin but not parvalbumin (91) and the "ventral division of the medioventral part of the posterior thalamus" with a similar profile of calcium binding proteins in mouse (92).

Based on the data obtained from injections of retrograde tracer into the PIL, identified by the presence of PTH2 neurons, the PIL receives significant ascending projections. These include direct projections from the contralateral spinal cord as well as indirect projections via the gracile and cuneate nuclei. The direct projections arise from throughout the thoracic and lumbar segments and mostly from neurons in deep layers of the dorsal horn of the spinal cord. Additional input arrives from the auditory cortex and the external cortex of the inferior colliculus, a non-tonotopically organized auditory nucleus with strong input from the auditory cortex and the spinal trigeminal nucleus (93, 94). In addition, the PIL also receives some descending input from the hypothalamus, particularly from the lateral preoptic area and the ventrolateral subdivision of the ventromedial hypothalamic nucleus. This pattern of PIL afferent connections is similar to that described for neuronal inputs to the parvicellular subparafascicular nucleus in male rats (95), where the ascending inputs were implicated in the processing of sensory information related to mating and ejaculation (96). Since the PIL includes the parvicellular subparafascicular nucleus, located ventromedial to the medial geniculate body, our results confirm previous data on the afferent neuronal connections of the PIL and expand the results to mother rats with injection sites verified by PTH2 double labeling.

PIL neurons project to several brain regions, such as the medial prefrontal cortex, lateral septum, amygdala, periaqueductal grey area and hypothalamus, including the medial preoptic area, the paraventricular, dorsomedial and ventromedial nuclei. These brain regions correspond to parts of the social brain network. The target regions of PIL neurons are also similar to the location of PTH2 fibers in the brain (89), suggesting that PTH2 neurons are the major projection neurons of the PIL.

5.2. Functional evidence of the role of the PIL and its PTH2-expressing neurons in the control of social behavior

The induction of PTH2 in response to social interaction generalizes previous findings on the elevated level of PTH2 in a mother rat in the presence of her litter (69). Furthermore, antagonizing PTH2R reduced the duration of social grooming, proving the role of PTH2-PTH2R system in the control of social behavior. These data are also in line with a recent report that the level of the corresponding peptide, PTH2, in individual zebrafish is proportional to the total density of zebrafish in the surrounding environment (81). In zebrafish, the cells expressing PTH2 were localized in a domain known to control the specification of diencephalic neuroendocrine cells (97). The site of socially dependent expression of PTH2 in mammals is the PIL (56), an area also defined recently in human based on molecular anatomy (98). The PIL corresponds to the area expressing PTH2 in the zebrafish based on the location of the cells.

While the results in the zebrafish study established how PTH2 expression is induced by conspecifics – using their lateral line organ to sense water vibrations elicited by their conspecifics (81), the actual function of PTH2 neurons, and PTH2 itself, remained unexplored. To address this question, we manipulated PIL neurons using chemogenetic tools in rats and found that the time spent social grooming was increased by chemogenetic stimulation of PIL neurons. Other types of social interactions, including sniffing or staying in the vicinity of each other when separated by walls were not affected. The physiological relevance of our finding is supported by reduced duration of social grooming following inhibition of the same PIL neurons. The same increase in the duration of social grooming was found when instead of chemogenetically stimulating all PIL neurons only those which were activated during a previous social interaction (socially tagged neurons) were stimulated, suggesting that promoting grooming between

individuals is dependent on socially activated neurons. Since social touch is rewarding (99), it is possible that a subset of social contact experienced neurons in the PIL promotes further social contact to maintain social interaction with conspecifics.

5.3. The PIL-PVN neuronal pathway and its characteristics

The high number of labeled neurons in the PIL following injection of retrograde tracer into the PVN suggests massive input of PIL neurons to the PVN. This pathway specifically connects the PIL with the PVN as neurons were not labeled outside the PIL. In turn, injections into brain areas adjacent to the PVN did not label the PIL. There have been several previous studies aimed at identification of the neuronal inputs to the PVN. Many of them failed to describe the PIL (33, 34, 100-103). We believe that the reasons include the previously poorly defined cyto- and chemoarchitecture of the area as well as the fact that it is situated at the border of the forebrain and the hindbrain where some sections can be lost during standard sectioning of the brain for anatomical mapping. Nevertheless, the projection from the PIL to the PVN has been previously reported using both retrograde and anterograde tracers (104). In that study the area projecting to the PVN was called the parvicellular division of the subparafascicular and posterior intralaminar nuclei. Thus, in the present study, we confirmed the existence of this pathway. We also showed that some of the PVN projecting cells contain PTH2. The results of the present study are also consistent with previous lesion studies that suggest hypothalamic projections from PIL PTH2 neurons (60, 105). The present study also showed that the retrogradely labeled neurons have an even distribution within the PIL, further suggesting that the PIL is a topographical unit, even though it does not correspond to an obvious cytoarchitectonically defined nucleus. Retrograde tracing from the PVN also demonstrated that PTH2 neurons constitute a significant portion of the projection neurons in the PIL. While PTH2 neurons contain calbindin, the majority of PVN-projecting PTH2-negative PIL cells are also calbindin-positive.

The immunolabeling proved that PTH2-containing neurons innervate oxytocin neurons in rats. In fact, the average of approximately 2 synaptic connections on the cell body and proxymal dendrites of PVN oxytocin neurons suggests a very robust action of PTH2 neurons on the oxytocin system. Indeed, the receptor for PTH2, the parathyroid hormone 2 receptor, has been previously shown to be particularly abundant in the PVN

(61, 76). PTH2 increases cAMP and Ca^{2+} levels by activating the PTH2 receptor *in vitro* (48), which suggests that the neuropeptide has an excitatory action. It is likely that the neurons that contain PTH2 also innervate oxytocin neurons when they do not contain a significant amount of PTH2, such as in non-maternal, e.g. nulliparous rats. It is likely that the PTH2 terminals use the excitatory amino acid transmitter glutamate. Thus, when PTH2 is not abundant in the terminals of PIL neurons (non-maternal animals), glutamate is still likely to be present and to exert an excitatory action on oxytocin neurons. Signaling by the PIL to oxytocin neurons in non-maternal animals may promote social behaviors via glutamate release. Co-released PTH2 may potentiate the effect of glutamate in maternal rats. While not addressed in this study, we speculate that PVN-projecting calbindin-positive but PTH2-negative neurons may also innervate oxytocin neurons, similar to PTH2 cells of the PIL, and also provide an excitatory input. PTH2-positive and -negative calbindin cells may be part of the same population with different strength of the PTH2 inducing stimulus. However, it cannot be exluded based on our results that they are different cell groups, which innervate different neuron populations in the PVN. Altogether, we firmly established the existence of an excitatory pathway that projects from the PIL to the PVN, and which is available to activate oxytocin neurons in lactating and also in non-lactating rats.

5.4. Potential functions of the PIL-oxytocin neuron connection

The PIL receives ascending input from the gracile and cuneate nuclei, which relay sensory information from the spinal cord through the dorsal fasciculus and medial lemniscus system. Direct spinal input also reaches the PIL, probably via collaterals of the spinothalamic tract. Both of these afferent connections are candidates to convey information from the somatosensory components of social contacts to the PIL. The PIL could also receive auditory input based on afferent connections from the external cortex of the inferior colliculus and the auditory cortex, and the previously reported activation of PTH2 neurons by auditory input (105). In the present study, the activation of calbindin neurons in the PIL was demonstrated in social context. Since the female rats were siblings and grew up together, their encounter in the familiar environment is not likely to evoke stress. Indeed, their extensive social interactions after reunion also argues against anxiety-induced activation of PIL calbindin neurons. In fact, previous c-fos studies in social

context focused on the social interaction of unfamiliar males in novel environment as an anxiety test (106-111). In these circumstances, a number of brain regions are activated but an increase in the number of c-Fos-positive cells in the area corresponding to the PIL was not reported. Thus, our study is the first to implicate the PIL in the adult brain social network. The activation of oxytocin neurons has been described in social context. In adult social contexts, oxytocin release and receptors contribute to social recognition and affiliative behavior (18, 19, 27, 32, 112, 113). Relevant to our model, i.c.v. oxytocin injection specifically increased huddling together in mice (114). Thus, we suggest that oxytocin neurons may be activated by the input from the PIL in different social situations in response to somatosensory, and possibly auditory stimuli from other animals. Thereby, the PIL-PVN pathway represents a previously missing link in the understanding of how oxytocin neurons can be activated by neuronal inputs.

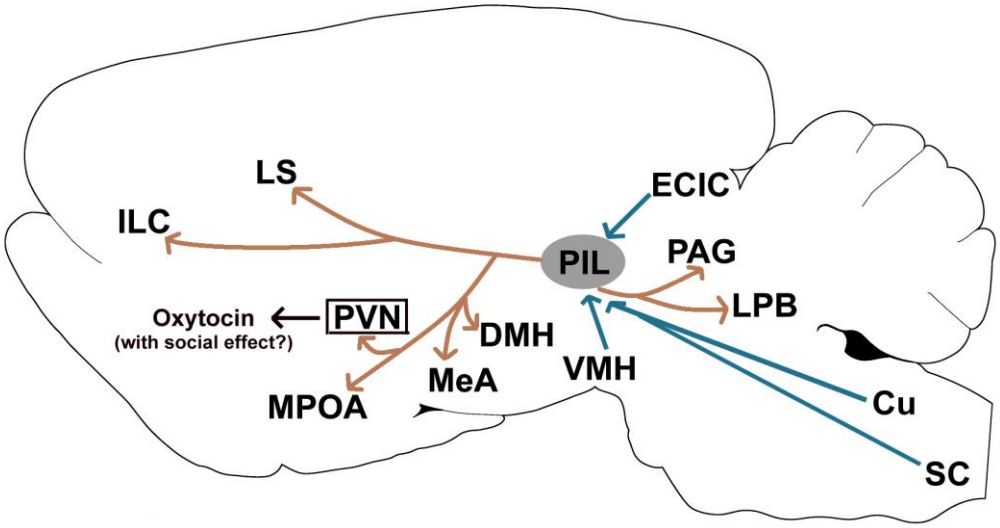

Figure 11. Schematic representation of the neuronal inputs and outputs of the posterior intralaminar complex of the thalamus (PIL).

Neurons in the spinal cord (SC), the cuneate (and gracile) nucleus (Cu), the external cortex of the inferior colliculus (ECIC), and the ventromedial hypothalamic nucleus (VMH) project to the PIL (blue arrows). Neurons in the PIL in turn project to the infralimbic cortex (ILC), the lateral septum (LS), the medial preoptic area (MPOA), the paraventricular hypothalamic nucleus (PVN), the medial amygdala (A), the dorsomedial hypothalamic nucleus (DMH) and the periaqueductal central grey (PAG) shown by brown arrows. Oxytocin neurons of the PVN may mediate the effect of the PIL on social behavior.

6. Conclusions

1. The PIL neurons project to different parts of the social brain network including the paraventricular nucleus of the hypothalamus.

2.. PIL neurons received ascending input from the spinal cord and inferior colliculus suggesting multimodal, e.g. somatosensory and auditory inputs.

3. PIL contained a high number of activated neurons in response to social encounter with an adult. The PIL neurons activated by social interaction contain calbindin.

4. Chemogenetic stimulation increased the activity of the PIL neurons expressing stimulatory receptors. Stimulation of PIL neurons evoked social grooming between conspecific animals.

5. Chemogenetic inhibition reduced social grooming behavior of female rats while control virus injected animals did not change their grooming behavior.

6. Stimulation and inhibition of PIL neurons, which were activated during previous social encounter, increased and decreased social grooming of the animals, respectively, without affecting their locomotor activity.

7. PTH2 is induced in the PIL region of thalamus in response to social interaction.

8. Antagonizing PTH2 receptor selectively inhibited social grooming.

9. Oxytocin neurons were closely apposed by an average of 2.0 and 0.4 PTH2 terminals in the PVN and the supraoptic nucleus, respectively.

10. Retrograde tracing identified PVN-projecting neurons in the PIL, many of which may be PTH2 neurons.

DOI:10.14753/SE.2023.2813

7. Summary

We discovered a novel neuronal pathway from the posterior intralaminar complex of the thalamus (PIL) to the paraventricular hypothalamic nucleus (PVN) and showed that the PIL neurons are involved in the control of social grooming. We provided evidence that the PIL contains relay neurons that convey stimuli from social partner via the spinal cord to oxytocin neurons of the PVN. We found that neurons in the PIL were activated by physical contact between female rats. In turn, chemogenetic stimulation and inhibition of PIL neurons increased and decreased social grooming behavior, respectively. Activity-dependent tagging of PIL neurons was performed in rats experiencing physical social contacts. Chemogenetic manipulation of these neurons also affected social grooming between familiar rats without altering locomotor activity. Neurons projecting from the PIL to the PVN express the neuropeptide parathyroid hormone 2 (PTH2) and central infusion of its receptor antagonist diminished social grooming. We propose that the discovered neuronal pathway facilitates physical contacts in mammals. Since the similarity of the PTH2-PTH2 receptor system between human and rodent has been demonstrated (115), the results may be relevant to human social interactions, too.

DOI:10.14753/SE.2023.2813

8. Magyar nyelvű összefoglalás (Summary in Hungarian)

Sikerült felfedeznünk egy új, a talamusz posterior intralamináris komplexumából (PIL) a hipotalamusz paraventricularis magjába (PVN) vetülő neuronális útvonalat, és megmutattuk, hogy a PIL neuronjai részt vesznek a direkt kontaktussal járó társas érintkezés szabályozásában. Bemutattuk, hogy a PIL átkapcsoló neuronjai aktiválódnak társas interakciók hatására, mely információt továbbíthatják a PVN oxitocin neuronjai felé. Megállapítottuk a PIL neuronjainak projekciós célterületeit, és hogy a PIL neuronjai aktiválódnak nőstény patkányok közötti fizikai kontaktus hatására. A PIL neuronok kemogenetikai stimulálása serkentette, míg gátlása csökkentette az egymás tisztogatásával, fizikai kontaktussal töltött időt. A PIL neuronok aktivitástól függő jelölését olyan patkányokon végeztük, melyekben mesterséges receptor csak olyan sejtekben fejeztünk ki, melyek korábban szociális interakció során aktiválódtak. Ezen neuronok kemogenetikai manipulálása szintén hasonló hatással volt az ismerős patkányok közötti direkt kontaktussal járó társas érintkezés idejére. A PIL-ből a PVN-be vetülő neuronok a parathormon 2-es neuropeptidet (PTH2) fejezik ki, és ezen neuropeptid receptorának antagonistájának agykamrai infúziója csökkentette a társas tisztálkodást. Eredményeink alapján feltételezhetjük, hogy a felfedezett neuronális útvonal serkenti az emlősök fizikai érintkezését. Mivel korábban már leírásra került a humán és rágcsáló PTH2-PTH2 receptor rendszere közötti hasonlóság (115), az eredmények relevánsak lehetnek az emberi társas interakciók szempontjából is.

9. References

1. Whishaw I, Bergdall V, Kolb B. Analysis of Behavior in Laboratory Rats. In: Suckow M, Weisbroth S, Franklin C (editor), The Laboratory Rat. Academic Press, eBook, 2006.

2. Rubenstein D, Rubenstein D. Social Behavior. In: Levin S (editor), Encyclopedia of Biodiversity Elsevier, Boston, 2013: 571-579.

3. O'Connell LA, Hofmann HA. (2011) The vertebrate mesolimbic reward system and social behavior network: a comparative synthesis. J Comp Neurol, 519: 3599-3639.

4. Newman SW. (1999) The medial extended amygdala in male reproductive behavior. A node in the mammalian social behavior network. Ann N Y Acad Sci, 877: 242-257.

5. Deco G, Rolls ET. (2005) Attention, short-term memory, and action selection: a unifying theory. Prog Neurobiol, 76: 236-256.

6. Wickens JR, Budd CS, Hyland BI, Arbuthnott GW. (2007) Striatal contributions to reward and decision making: making sense of regional variations in a reiterated processing matrix. Ann N Y Acad Sci, 1104: 192-212.

7. Schweinfurth MK. (2020) The social life of Norway rats (Rattus norvegicus). eLife, 9.

8. Monfils MH, Agee LA. (2019) Insights from social transmission of information in rodents. Genes Brain Behav, 18: e12534.

9. Ellingsen DM, Leknes S, Loseth G, Wessberg J, Olausson H. (2015) The Neurobiology Shaping Affective Touch: Expectation, Motivation, and Meaning in the Multisensory Context. Frontiers in psychology, 6: 1986.

10. Ebbesen CL, Froemke RC. (2021) Body language signals for rodent social communication. Current opinion in neurobiology, 68: 91-106.

11. Zilkha N, Sofer Y, Kashash Y, Kimchi T. (2021) The social network: Neural control of sex differences in reproductive behaviors, motivation, and response to social isolation. Current opinion in neurobiology, 68: 137-151.

12. Ahmadlou M, Houba JHW, van Vierbergen JFM, Giannouli M, Gimenez GA, van Weeghel C, Darbanfouladi M, Shirazi MY, Dziubek J, Kacem M, de Winter F, Heimel JA. (2021) A cell type-specific cortico-subcortical brain circuit for investigatory and novelty-seeking behavior. Science, 372.

13. Burbach JPH, Young LJ, Russell JA. Oxytocin: Synthesis, Secretion, and Reproductive Functions. In: Neill JD (editor), Knobil and Neill´s Physiology of Reproduction. Academic Press, Oxford, 2006.

14. Leng G, Meddle SL, Douglas AJ. (2008) Oxytocin and the maternal brain. Current opinion in pharmacology, 8: 731-734.

15. Rich ME, deCardenas EJ, Lee HJ, Caldwell HK. (2014) Impairments in the initiation of maternal behavior in oxytocin receptor knockout mice. PloS one, 9: e98839.

16. Bosch OJ, Neumann ID. (2012) Both oxytocin and vasopressin are mediators of maternal care and aggression in rodents: from central release to sites of action. Hormones and behavior, 61: 293-303.

17. Marlin BJ, Mitre M, D'Amour J A, Chao MV, Froemke RC. (2015) Oxytocin enables maternal behaviour by balancing cortical inhibition. Nature, 520: 499-504.

18. Strathearn L, Fonagy P, Amico J, Montague PR. (2009) Adult attachment predicts maternal brain and oxytocin response to infant cues. Neuropsychopharmacology, 34: 2655-2666.

19. Neumann ID. (2008) Brain oxytocin: a key regulator of emotional and social behaviours in both females and males. J Neuroendocrinol, 20: 858-865.

20. Numan M, Young LJ. (2016) Neural mechanisms of mother-infant bonding and pair bonding: Similarities, differences, and broader implications. Hormones and behavior, 77: 98-112.

21. Tang Y, Benusiglio D, Lefevre A, Hilfiger L, Althammer F, Bludau A, Hagiwara D, Baudon A, Darbon P, Schimmer J, Kirchner MK, Roy RK, Wang S, Eliava M, Wagner S, Oberhuber M, Conzelmann KK, Schwarz M, Stern JE, Leng G, Neumann ID, Charlet A, Grinevich V. (2020) Social touch promotes interfemale communication via activation of parvocellular oxytocin neurons. Nature neuroscience, 23: 1125-1137.

22. Knobloch HS, Grinevich V. (2014) Evolution of oxytocin pathways in the brain of vertebrates. Frontiers in behavioral neuroscience, 8: 31.

23. Bealer SL, Armstrong WE, Crowley WR. (2010) Oxytocin release in magnocellular nuclei: neurochemical mediators and functional significance during gestation. Am J Physiol Regul Integr Comp Physiol, 299: R452-458.

24. Russell JA, Leng G, Douglas AJ. (2003) The magnocellular oxytocin system, the fount of maternity: adaptations in pregnancy. Front Neuroendocrinol, 24: 27-61.

25. Grinevich V, Knobloch-Bollmann HS, Eliava M, Busnelli M, Chini B. (2016) Assembling the Puzzle: Pathways of Oxytocin Signaling in the Brain. Biological psychiatry, 79: 155-164.

26. Mitre M, Marlin BJ, Schiavo JK, Morina E, Norden SE, Hackett TA, Aoki CJ, Chao MV, Froemke RC. (2016) A Distributed Network for Social Cognition Enriched for Oxytocin Receptors. J Neurosci, 36: 2517-2535.

27. Feldman R, Monakhov M, Pratt M, Ebstein RP. (2016) Oxytocin Pathway Genes: Evolutionary Ancient System Impacting on Human Affiliation, Sociality, and Psychopathology. Biological psychiatry, 79: 174-184.

28. Romano A, Tempesta B, Micioni Di Bonaventura MV, Gaetani S. (2015) From Autism to Eating Disorders and More: The Role of Oxytocin in Neuropsychiatric Disorders. Front Neurosci, 9: 497.

29. Lee MR, Rohn MC, Tanda G, Leggio L. (2016) Targeting the Oxytocin System to Treat Addictive Disorders: Rationale and Progress to Date. CNS drugs, 30: 109-123.

30. Lefevre A, Sirigu A. (2016) The two fold role of oxytocin in social developmental disorders: A cause and a remedy? Neuroscience and biobehavioral reviews, 63: 168-176.

31. Brown CH, Bains JS, Ludwig M, Stern JE. (2013) Physiological regulation of magnocellular neurosecretory cell activity: integration of intrinsic, local and afferent mechanisms. J Neuroendocrinol, 25: 678-710.

32. Ross HE, Young LJ. (2009) Oxytocin and the neural mechanisms regulating social cognition and affiliative behavior. Front Neuroendocrinol, 30: 534-547.

33. Pan B, Castro-Lopes JM, Coimbra A. (1999) Central afferent pathways conveying nociceptive input to the hypothalamic paraventricular nucleus as revealed by a combination of retrograde labeling and c-fos activation. J Comp Neurol, 413: 129-145.

34. Larsen PJ, Mikkelsen JD. (1995) Functional identification of central afferent projections conveying information of acute "stress" to the hypothalamic paraventricular nucleus. J Neurosci, 15: 2609-2627.

35. Leng G, Brown CH, Russell JA. (1999) Physiological pathways regulating the activity of magnocellular neurosecretory cells. Prog Neurobiol, 57: 625-655.

36. Li C, Chen P, Smith MS. (1999) Neural populations in the rat forebrain and brainstem activated by the suckling stimulus as demonstrated by cFos expression. Neuroscience, 94: 117-129.

37. Tindal JS. (1972) Reflex pathways controlling lactation. Proceedings of the Royal Society of Medicine, 65: 1085-1086.

38. Knaggs GS, McNeilly AS, Tindal JS. (1972) The afferent pathway of the milk-ejection reflex in the mid-brain of the goat. The Journal of endocrinology, 52: 333-341.

39. Wang YF, Negoro H, Honda K. (1995) Effects of hemitransection of the midbrain on milk-ejection burst of oxytocin neurones in lactating rat. The Journal of endocrinology, 144: 463-470.

40. Dubois-Dauphin M, Armstrong WE, Tribollet E, Dreifuss JJ. (1985) Somatosensory systems and the milk-ejection reflex in the rat. II. The effects of lesions in the ventroposterior thalamic complex, dorsal columns and lateral cervical nucleus-dorsolateral funiculus. Neuroscience, 15: 1131-1140.

41. Dubois-Dauphin M, Armstrong WE, Tribollet E, Dreifuss JJ. (1985) Somatosensory systems and the milk-ejection reflex in the rat. I. Lesions of the mesencephalic lateral tegmentum disrupt the reflex and damage mesencephalic somatosensory connections. Neuroscience, 15: 1111-1129.

42. Hansen S, Kohler C. (1984) The importance of the peripeduncular nucleus in the neuroendocrine control of sexual behavior and milk ejection in the rat. Neuroendocrinology, 39: 563-572.

43. Cservenak M, Keller D, Kis V, Fazekas EA, Ollos H, Leko AH, Szabo ER, Renner E, Usdin TB, Palkovits M, Dobolyi A. (2017) A Thalamo-Hypothalamic Pathway That Activates Oxytocin Neurons in Social Contexts in Female Rats. Endocrinology, 158: 335-348.

44. Dávid Keller TL, Melinda Cservenák, Gina Puska, János Barna, Veronika Csillag, Imre Farkas, Dóra Zelena, Fanni Dóra, Lara Barteczko, Ted B. Usdin, Miklós Palkovits, Mazahir T. Hasan, Valery Grinevich, Arpád Dobolyi. (2022) A thalamo-preoptic pathway promoting social touch. bioRxiv, doi:https://doi.org/10.1101/2022.01.11.475648.

45. Usdin TB, Gruber C, Bonner TI. (1995) Identification and functional expression of a receptor selectively recognizing parathyroid hormone, the PTH2 receptor. J Biol Chem, 270: 15455-15458.

46. Usdin TB, Bonner TI, Hoare SR. (2002) The parathyroid hormone 2 (PTH2) receptor. Receptors Channels, 8: 211-218.

47. Usdin TB, Hoare SR, Wang T, Mezey E, Kowalak JA. (1999) TIP39: a new neuropeptide and PTH2-receptor agonist from hypothalamus. Nature neuroscience, 2: 941-943.

48. Goold CP, Usdin TB, Hoare SR. (2001) Regions in rat and human parathyroid hormone (PTH) 2 receptors controlling receptor interaction with PTH and with antagonist ligands. J Pharmacol Exp Ther, 299: 678-690.

49. Della Penna K, Kinose F, Sun H, Koblan KS, Wang H. (2003) Tuberoinfundibular peptide of 39 residues (TIP39): molecular structure and activity for parathyroid hormone 2 receptor. Neuropharmacology, 44: 141-153.

50. Piserchio A, Usdin T, Mierke DF. (2000) Structure of tuberoinfundibular peptide of 39 residues. J Biol Chem, 275: 27284-27290.

51. Usdin TB, Bonner TI, Harta G, Mezey E. (1996) Distribution of parathyroid hormone-2 receptor messenger ribonucleic acid in rat. Endocrinology, 137: 4285-4297.

52. Hoare SR, Bonner TI, Usdin TB. (1999) Comparison of rat and human parathyroid hormone 2 (PTH2) receptor activation: PTH is a low potency partial agonist at the rat PTH2 receptor. Endocrinology, 140: 4419-4425.

53. Clark JA, Bonner TI, Kim AS, Usdin TB. (1998) Multiple regions of ligand discrimination revealed by analysis of chimeric parathyroid hormone 2 (PTH2) and PTH/PTH-related peptide (PTHrP) receptors. Molecular endocrinology (Baltimore, Md, 12: 193-206.

54. Hoare SR, Clark JA, Usdin TB. (2000) Molecular determinants of tuberoinfundibular peptide of 39 residues (TIP39) selectivity for the parathyroid hormone-2 (PTH2) receptor. N-terminal truncation of TIP39 reverses PTH2 receptor/PTH1 receptor binding selectivity. J Biol Chem, 275: 27274-27283.

55. Kuo J, Usdin TB. (2007) Development of a rat parathyroid hormone 2 receptor antagonist. Peptides, 28: 887-892.

56. Dobolyi A, Palkovits M, Usdin TB. (2010) The TIP39-PTH2 receptor system: unique peptidergic cell groups in the brainstem and their interactions with central regulatory mechanisms. Prog Neurobiol, 90: 29-59.

57. Dobolyi A, Cservenak M, Young LJ. (2018) Thalamic integration of social stimuli regulating parental behavior and the oxytocin system. Front Neuroendocrinol, 51: 102-115.

58. Brenner D, Bago AG, Gallatz K, Palkovits M, Usdin TB, Dobolyi A. (2008) Tuberoinfundibular peptide of 39 residues in the embryonic and early postnatal rat brain. J Chem Neuroanat, 36: 59-68.

59. Cservenak M, Szabo ER, Bodnar I, Leko A, Palkovits M, Nagy GM, Usdin TB, Dobolyi A. (2013) Thalamic neuropeptide mediating the effects of nursing on lactation and maternal motivation. Psychoneuroendocrinology, 38: 3070-3084.

60. Dobolyi A, Palkovits M, Bodnar I, Usdin TB. (2003) Neurons containing tuberoinfundibular peptide of 39 residues project to limbic, endocrine, auditory and spinal areas in rat. Neuroscience, 122: 1093-1105.

61. Faber CA, Dobolyi A, Sleeman M, Usdin TB. (2007) Distribution of tuberoinfundibular peptide of 39 residues and its receptor, parathyroid hormone 2 receptor, in the mouse brain. J Comp Neurol, 502: 563-583.

62. Hokfelt T, Phillipson O, Goldstein M. (1979) Evidence for a dopaminergic pathway in the rat descending from the A11 cell group to the spinal cord. Acta Physiol Scand, 107: 393-395.

63. Nandi D, Aziz T, Carter H, Stein J. (2003) Thalamic field potentials in chronic central pain treated by periventricular gray stimulation -- a series of eight cases. Pain, 101: 97-107.

64. Dobolyi A, Irwin S, Makara G, Usdin TB, Palkovits M. (2005) Calcitonin gene-related peptide-containing pathways in the rat forebrain. J Comp Neurol, 489: 92-119.

65. Barsy B, Kocsis K, Magyar A, Babiczky A, Szabo M, Veres JM, Hillier D, Ulbert I, Yizhar O, Matyas F. (2020) Associative and plastic thalamic signaling to the lateral amygdala controls fear behavior. Nature neuroscience, 23: 625-637.

66. Coolen LM, Veening JG, Petersen DW, Shipley MT. (2003) Parvocellular subparafascicular thalamic nucleus in the rat: anatomical and functional compartmentalization. J Comp Neurol, 463: 117-131.

67. Varga T, Palkovits M, Usdin TB, Dobolyi A. (2008) The medial paralemniscal nucleus and its afferent neuronal connections in rat. J Comp Neurol, 511: 221-237.

68. Fenzl T, Schuller G. (2002) Periaqueductal gray and the region of the paralemniscal area have different functions in the control of vocalization in the neotropical bat, Phyllostomus discolor. Eur J Neurosci, 16: 1974-1986.

69. Cservenak M, Bodnar I, Usdin TB, Palkovits M, Nagy GM, Dobolyi A. (2010) Tuberoinfundibular peptide of 39 residues is activated during lactation and participates in the suckling-induced prolactin release in rat. Endocrinology, 151: 5830-5840.

70. Varga T, Mogyorodi B, Bago AG, Cservenak M, Domokos D, Renner E, Gallatz K, Usdin TB, Palkovits M, Dobolyi A. (2012) Paralemniscal TIP39 is induced in rat dams and may participate in maternal functions. Brain Struct Funct, 217: 323-335.

71. Coutellier L, Logemann A, Rusnak M, Usdin TB. (2011) Maternal absence of the parathyroid hormone 2 receptor affects postnatal pup development. J Neuroendocrinol, 23: 612-619.

72. Brown RSE, Aoki M, Ladyman SR, Phillipps HR, Wyatt A, Boehm U, Grattan DR. (2017) Prolactin action in the medial preoptic area is necessary for postpartum maternal nursing behavior. Proc Natl Acad Sci U S A, 114: 10779-10784.

73. Pereira M. (2016) Structural and Functional Plasticity in the Maternal Brain Circuitry. New directions for child and adolescent development, 2016: 23-46.

74. Olah S, Cservenak M, Keller D, Fazekas EA, Renner E, Low P, Dobolyi A. (2018) Prolactin-induced and neuronal activation in the brain of mother mice. Brain structure & function, 223: 3229-3250.

75. Bridges RS. (2020) The behavioral neuroendocrinology of maternal behavior: Past accomplishments and future directions. Hormones and behavior, 120: 104662.

76. Dobolyi A, Irwin S, Wang J, Usdin TB. (2006) The distribution and neurochemistry of the parathyroid hormone 2 receptor in the rat hypothalamus. Neurochem Res, 31: 227-236.

77. Wu Z, Autry AE, Bergan JF, Watabe-Uchida M, Dulac CG. (2014) Galanin neurons in the medial preoptic area govern parental behaviour. Nature, 509: 325-330.

78. Cservenak M, Kis V, Keller D, Dimen D, Menyhart L, Olah S, Szabo ER, Barna J, Renner E, Usdin TB, Dobolyi A. (2017) Maternally involved galanin neurons in the preoptic area of the rat. Brain Struct Funct, 222: 781-798.

79. Scott N, Prigge M, Yizhar O, Kimchi T. (2015) A sexually dimorphic hypothalamic circuit controls maternal care and oxytocin secretion. Nature, 525: 519-522.

80. Moffitt JR, Bambah-Mukku D, Eichhorn SW, Vaughn E, Shekhar K, Perez JD, Rubinstein ND, Hao J, Regev A, Dulac C, Zhuang X. (2018) Molecular, spatial, and functional single-cell profiling of the hypothalamic preoptic region. Science, 362.

81. Anneser L, Alcantara IC, Gemmer A, Mirkes K, Ryu S, Schuman EM. (2020) The neuropeptide Pth2 dynamically senses others via mechanosensation. Nature, 588: 653-657.

82. Bankhead P, Loughrey MB, Fernandez JA, Dombrowski Y, McArt DG, Dunne PD, McQuaid S, Gray RT, Murray LJ, Coleman HG, James JA, Salto-Tellez M, Hamilton PW. (2017) QuPath: Open source software for digital pathology image analysis. Sci Rep, 7: 16878.

83. Dobolyi A, Ueda H, Uchida H, Palkovits M, Usdin TB. (2002) Anatomical and physiological evidence for involvement of tuberoinfundibular peptide of 39 residues in nociception. Proc Natl Acad Sci U S A, 99: 1651-1656.

84. Wang J, Palkovits M, Usdin TB, Dobolyi A. (2006) Forebrain projections of tuberoinfundibular peptide of 39 residues (TIP39)-containing subparafascicular neurons. Neuroscience, 138: 1245-1263.

85. Dobolyi A. (2009) Central amylin expression and its induction in rat dams. J Neurochem, 111: 1490-1500.

86. Paxinos G, Watson C. The rat brain in stereotaxic coordinates. Academic Press, San Diego, 2007.

87. Hasan MT, Althammer F, Silva da Gouveia M, Goyon S, Eliava M, Lefevre A, Kerspern D, Schimmer J, Raftogianni A, Wahis J, Knobloch-Bollmann HS, Tang Y, Liu X, Jain A, Chavant V, Goumon Y, Weislogel JM, Hurlemann R, Herpertz SC, Pitzer C, Darbon P, Dogbevia GK, Bertocchi I, Larkum ME, Sprengel R, Bading H, Charlet A, Grinevich V. (2019) A Fear Memory Engram and Its Plasticity in the Hypothalamic Oxytocin System. Neuron, 103: 133-146.

88. Keller D, Tsuda MC, Usdin TB, Dobolyi A. (2022) Behavioural actions of tuberoinfundibular peptide 39 (parathyroid hormone 2). J Neuroendocrinol, 34: e13130.

89. Dobolyi A, Palkovits M, Usdin TB. (2003) Expression and distribution of tuberoinfundibular peptide of 39 residues in the rat central nervous system. J Comp Neurol, 455: 547-566.

90. Rogers JH, Resibois A. (1992) Calretinin and calbindin-D28k in rat brain: patterns of partial co-localization. Neuroscience, 51: 843-865.

91. Cruikshank SJ, Killackey HP, Metherate R. (2001) Parvalbumin and calbindin are differentially distributed within primary and secondary subregions of the mouse auditory forebrain. Neuroscience, 105: 553-569.

92. Motomura K, Kosaka T. (2011) Medioventral part of the posterior thalamus in the mouse. J Chem Neuroanat, 42: 192-209.

93. Herbert H, Aschoff A, Ostwald J. (1991) Topography of projections from the auditory cortex to the inferior colliculus in the rat. J Comp Neurol, 304: 103-122.

94. Zhou J, Shore S. (2006) Convergence of spinal trigeminal and cochlear nucleus projections in the inferior colliculus of the guinea pig. J Comp Neurol, 495: 100-112.

95. Coolen LM, Veening JG, Wells AB, Shipley MT. (2003) Afferent connections of the parvocellular subparafascicular thalamic nucleus in the rat: evidence for functional subdivisions. J Comp Neurol, 463: 132-156.

96. Coolen LM, Allard J, Truitt WA, McKenna KE. (2004) Central regulation of ejaculation. Physiol Behav, 83: 203-215.

97. Fernandes AM, Beddows E, Filippi A, Driever W. (2013) Orthopedia transcription factor otpa and otpb paralogous genes function during dopaminergic and neuroendocrine cell specification in larval zebrafish. PloS one, 8: e75002.

98. Nagalski A, Puelles L, Dabrowski M, Wegierski T, Kuznicki J, Wisniewska MB. (2016) Molecular anatomy of the thalamic complex and the underlying transcription factors. Brain Struct Funct, 221: 2493-2510.

99. Shamay-Tsoory SG, Eisenberger NI. (2021) Getting in touch: A neural model of comforting touch. Neuroscience and biobehavioral reviews, 130: 263-273.

100. Kiss JZ, Palkovits M, Zaborszky L, Tribollet E, Szabo D, Makara GB. (1983) Quantitative histological studies on the hypothalamic paraventricular nucleus in rats. II. Number of local and certain afferent nerve terminals. Brain Res, 265: 11-20.

101. Qi Y, Namavar MR, Iqbal J, Oldfield BJ, Clarke IJ. (2009) Characterization of the projections to the hypothalamic paraventricular and periventricular nuclei in the female sheep brain, using retrograde tracing and immunohistochemistry. Neuroendocrinology, 90: 31-53.

102. Csaki A, Kocsis K, Halasz B, Kiss J. (2000) Localization of glutamatergic/aspartatergic neurons projecting to the hypothalamic paraventricular nucleus studied by retrograde transport of [3H]D-aspartate autoradiography. Neuroscience, 101: 637-655.

103. Larsen PJ, Hay-Schmidt A, Vrang N, Mikkelsen JD. (1996) Origin of projections from the midbrain raphe nuclei to the hypothalamic paraventricular nucleus in the rat: a combined retrograde and anterograde tracing study. Neuroscience, 70: 963-988.

104. Campeau S, Watson SJ, Jr. (2000) Connections of some auditory-responsive posterior thalamic nuclei putatively involved in activation of the hypothalamo-pituitary-adrenocortical axis in response to audiogenic stress in rats: an anterograde and retrograde tract tracing study combined with Fos expression. J Comp Neurol, 423: 474-491.

105. Palkovits M, Helfferich F, Dobolyi A, Usdin TB. (2009) Acoustic stress activates tuberoinfundibular peptide of 39 residues neurons in the rat brain. Brain Struct Funct, 214: 15-23.

106. Salchner P, Lubec G, Singewald N. (2004) Decreased social interaction in aged rats may not reflect changes in anxiety-related behaviour. Behav Brain Res, 151: 1-8.

107. Young LJ. (2002) The neurobiology of social recognition, approach, and avoidance. Biological psychiatry, 51: 18-26.

108. Fleming AS, Suh EJ, Korsmit M, Rusak B. (1994) Activation of Fos-like immunoreactivity in the medial preoptic area and limbic structures by maternal and social interactions in rats. Behavioral neuroscience, 108: 724-734.

109. File SE, Seth P. (2003) A review of 25 years of the social interaction test. Eur J Pharmacol, 463: 35-53.

110. Martinez M, Phillips PJ, Herbert J. (1998) Adaptation in patterns of c-fos expression in the brain associated with exposure to either single or repeated social stress in male rats. Eur J Neurosci, 10: 20-33.

111. Jodo E, Katayama T, Okamoto M, Suzuki Y, Hoshino K, Kayama Y. (2010) Differences in responsiveness of mediodorsal thalamic and medial prefrontal cortical neurons to social interaction and systemically administered phencyclidine in rats. Neuroscience, 170: 1153-1164.

112. Ferguson JN, Young LJ, Hearn EF, Matzuk MM, Insel TR, Winslow JT. (2000) Social amnesia in mice lacking the oxytocin gene. Nature genetics, 25: 284-288.

113. Kent P, Awadia A, Zhao L, Ensan D, Silva D, Cayer C, James JS, Anisman H, Merali Z. (2016) Effects of intranasal and peripheral oxytocin or gastrin-releasing peptide administration on social interaction and corticosterone levels in rats. Psychoneuroendocrinology, 64: 123-130.

114. Arakawa H, Blanchard DC, Blanchard RJ. (2015) Central oxytocin regulates social familiarity and scent marking behavior that involves amicable odor signals between male mice. Physiol Behav, 146: 36-46.

115. Bago AG, Dimitrov E, Saunders R, Seress L, Palkovits M, Usdin TB, Dobolyi A. (2009) Parathyroid hormone 2 receptor and its endogenous ligand tuberoinfundibular peptide of 39 residues are concentrated in endocrine, viscerosensory and auditory brain regions in macaque and human. Neuroscience, 162: 128-147.

10. Bibliography of the candidate's publications

Publications related to this dissertation

1. **Keller D**, Tsuda MC, Usdin TB, Dobolyi A (2022) The behavioural actions of tuberoinfundibular peptide 39 (parathyroid hormone 2). *Journal of Neuroendocrinology*, 34:e13130. (IF: 3.870).
2. *Cservenák M, ***Keller D**, Kis V, Fazekas EA, Öllös H, Lékó A, Szabó ER, Renner E, Usdin TB, Palkovits M, Dobolyi A (2017) A thalamo-hypothalamic pathway that activates oxytocin neurons in social contexts in female rats. *Endocrinology*, 158:335-348. (IF: 3.961). ***: equal contribution.**

Publications not included in the dissertation:

1. **Keller D**, Láng T, Cservenák M, Puska G, Barna J, Csillag V, Farkas I, Zelena D, Dóra F, Küppers S, Barteczko L, Usdin TB, Palkovits M, Hasan MT, Grinevich V, Dobolyi A (2022) A thalamo-preoptic pathway promotes social grooming in rodents. *Current Biology*, provisionally accepted (IF: 10.900; manuscript number: D-22-01361), bioRxiv. 2022; doi:https://doi.org/10.1101/2022.01.11.475648.
2. Dóra F, Renner É, **Keller D**, Palkovits M, Dobolyi A (2022) Transcriptome Profiling of the Dorsomedial Prefrontal Cortex in Suicide Victims. *International Journal of Molecular Science*, 23:7067. (IF: 6.208)
3. Gelencsér-Horváth A, Kopácsi L, Varga V, **Keller D**, Dobolyi Á, Karacs K, Lőrincz A (2022) Tracking Highly Similar Rat Instances under Heavy Occlusions: An Unsupervised Deep Generative Pipeline. *Journal of Imaging*, 8:109.
4. Lékó AH, Kumari R, Dóra F, **Keller D**, Udvari EB, Csikós V, Renner E, Dobolyi A (2021) Transcriptome Sequencing in the Preoptic Region of Rat Dams Reveals a Role of Androgen Receptor in the Control of Maternal Behavior. *International Journal of Molecular Sciences*, 22:1517. (IF: 6.208)
5. Dobolyi A, Oláh S, **Keller D**, Rashmi Kumari, Fazekas EA, Csikós V, Renner E, Cservenák M (2020) Secretion and function of pituitary prolactin in evolutionary perspective. *Frontiers in Neuroscience*, 14:621. (IF: 4.677)
6. Oláh Sz, Cservenák M, **Keller D**, Fazekas EA, Renner E, Lőw P, Dobolyi A (2018) Prolactin-induced and neuronal activation in the brain of mother mice. *Brain*

Structure and Function, 223:3229-3250. (IF: 3.622)

7. Cservenák M, Kis V, **Keller D**, Dimén D, Menyhárt L, Oláh S, Szabó ER, Barna J, Renner E, Usdin TB, Dobolyi A (2017) Maternally involved galanin neurons in the preoptic area of the rat. *Brain Structure and Function,* 222:781-798. (IF: 4.231)

Oral presentation at international conferences

1. **Dávid Keller** (2022) A thalamo-preoptic pathway promoting social touch. IBNS (is) Staying Connected, International Behavioral Neuroscience Society, online.
2. **Dávid Keller** (2022) A thalamo-preoptic pathway promoting social touch. The (European) Social Club Initiative, online.
3. **Dávid Keller**, Tamás Láng, Melinda Cservenák, Arpád Dobolyi (2021) A New Brain Mechanism Promoting Physical Contact in Social Behaviour. Semmelweis University, PhD Scientific Days, Budapest, Hungary.
4. **Dávid Keller**, Tamás Láng, Melinda Cservenák, Emese A. Fazekas, Arpád Dobolyi (2020) A novel thalamo-preoptic neuronal pathway affects social interaction in rat. Subcortical neural processing of saliency, virtual symposium.
5. **Dávid Keller**, Tamás Láng, Melinda Cservenák, Emese A. Fazekas, Arpád Dobolyi (2020) Involvement of a Novel Thalamo-Preoptic Neuronal Pathway in Social Interaction Using Double Viral Chemogenetics in the Rat. Semmelweis University, PhD Scientific Days, Budapest, Hungary.
6. **Dávid Keller**, Emese A. Fazekas, Árpád Dobolyi (2019) Chemogenetic evidence of a thalamic pathway conveying social input from a conspecific to higher brain centers in rat. European Neuroscience Conference for Doctoral Students (ENCODS), London, United Kingdom.
7. **Dávid Keller**, Emese A. Fazekas, Árpád Dobolyi (2019) Chemogenetic evidence of a novel neuronal pathway conveying social input from a conspecific to higher brain centers in rat. Semmelweis University, PhD Scientific Days, Budapest, Hungary.
8. **Dávid Keller**, Melinda Cservenák, Viktor Kis, Emese A. Fazekas, Hanna Öllös, András Lékó, Éva R. Szabó, Éva Renner, Ted B. Usdin, Miklós Palkovits, Árpád Dobolyi (2017) A new thalamo-hypothalamic pathway that activates oxytocin neurons. 49th Annual Scientific Meeting of the Hungarian Medical Association of

America, Sarasota, USA.

9. **Dávid Keller**, Melinda Cservenák, Viktor Kis, Emese A. Fazekas, Hanna Öllös, András Lékó, Éva R. Szabó, Éva Renner, Ted B. Usdin, Miklós Palkovits, Árpád Dobolyi (2017) A thalamo-hypothalamic pathway that activates oxytocin neurons in social contexts in the rat. In4Med Coimbra's Scientific and Medical Congress, Portugal.

Poster presentation at international conferences

1. **Dávid Keller,** Tamás Láng, Melinda Cservenák, Gina Puska, János Barna, Veronika Csillag, Imre Farkas, Dóra Zelena, Fanni Dóra, Lara Barteczko, Ted B. Usdin, Miklós Palkovits, Mazahir T. Hasan, Valery Grinevich, Arpád Dobolyi (2022) A thalamo-preoptic pathway promoting social touch. FENS Forum 2022, Paris, France.
2. **Dávid Keller**, Tamás Láng, Melinda Cservenák, Gina Puska, János Barna, Arpád Dobolyi (2022) A thalamo-preoptic pathway promoting social touch. 45th Annual Meeting of the Japan Neuroscience Society (NEURO2022), Okinawa, Japan.
3. **Dávid Keller**, Tamás Láng, Melinda Cservenák, Gina Puska, János Barna, Arpád Dobolyi (2022) A new brain mechanism promoting physical contact in social behaviour. IBRO Workshop Budapest 2022.
4. **Dávid Keller**, Tamás Láng, Melinda Cservenák, Arpád Dobolyi (2021) A New Brain Mechanism Promoting Physical Contact in Social Behaviour. Social Behavior Symposium, Alicante, Spain.
5. **Dávid Keller**, Tamás Láng, Melinda Cservenák, Arpád Dobolyi (2021) Subcortical control of behavior by direct social contact. 49th Meeting of the European Brain and Behaviour Society (EBBS), Lausanne, Switzerland.
6. **Dávid Keller**, Tamás Láng, Melinda Cservenák, Arpád Dobolyi (2021) Subcortical control of behavior by direct social contact. 30th Annual meeting of the International Behavioral Neuroscience Society (IBNS), Puerto Vallarta, Mexico.
7. **Dávid Keller**, Tamás Láng, Melinda Cservenák, Emese A. Fazekas, Arpád Dobolyi (2020) Involvement of a novel thalamo-preoptic neuronal pathway in social interaction using chemogenetics in rat. 29th Annual meeting of the International Behavioral Neuroscience Society (IBNS), virtual conference.

8. **Dávid Keller**, Tamás Láng, Melinda Cservenák, Emese A. Fazekas, Arpád Dobolyi (2020) Chemogenetics Establishes a Novel Thalamo-Hypothalamic Pathway Conveying Social Information on Direct Contact to the Preoptic Area. 12th Forum of Neuroscience (FENS), virtual conference.
9. **Dávid Keller**, Tamás Láng, Melinda Cservenák, Emese A. Fazekas, Arpád Dobolyi (2020) Chemogenetic analysis of an ascending thalamic pathway conveying social information of conspecific rats. IBRO Workshop Budapest 2020, Szeged, Hungary.
10. **Dávid Keller**, Emese A. Fazekas, Árpád Dobolyi (2019) A thalamic complex specifically involved in social behavior based on chemogenetic evidence in the rat. International Brain Research Organisation (IBRO) 10th World Congress of Neuroscience, Daegu, Korea.
11. **Dávid Keller**, Emese A. Fazekas, Árpád Dobolyi (2019) Chemogenetic evidence of a novel neuronal pathway conveying social input from a conspecific to higher brain centers in rat. FENS Regional Meeting, Belgrade, Serbia.
12. **Dávid Keller**, Emese A. Fazekas, Árpád Dobolyi (2019) Chemogenetics reveals a novel neuronal pathway mediating inputs related to social behaviour in rat. FAMÉ 2019, Budapest, Hungary. (Poster Award of Youth Section)
13. **Dávid Keller**, Melinda Cservenák, Emese A. Fazekas, Árpád Dobolyi (2018) The TIP39 neuropeptide system as a drug target in autism by its ability to influence oxytocin secretion. Chemistry towards Biology (CTB9), Budapest, Hungary. (2nd prize)
14. **Dávid Keller**, Melinda Cservenák, Viktor Kis, Emese A. Fazekas, András Lékó, Miklós Palkovits, Árpád Dobolyi (2018) A thalamo-hypothalamic projection that may activate oxytocin neurons in response to social interaction. Abstract Book: 3334. 11th Forum of Neuroscience (FENS), Berlin, Germany.
15. **Keller Dávid**, Cservenák Melinda, Kis Viktor, Szabó Éva R., Dobolyi Árpád (2016): The neuronal pathway that activates oxytocin neurons during parturition in mother rats. Program and Abstract Book: 260-261. IBRO Workshop Budapest 2016, Hungary.
16. Cservenák Melinda, **Keller Dávid**, Kis Viktor, Barna János, Szabó Éva R. Dobolyi Árpád (2016): Prolactin responsive galanin neurons in the medial preoptic area of

mother rats. Program and Abstract Book: 261-262. IBRO Workshop Budapest 2016, Hungary

First author presentation at national scientific and students' conferences

1. 21st Congress of the Hungarian Anatomical Society, 2021
2. The Association of Hungarian PhD and DLA Candidates - Science and Innovation Conference, Neuroscience section, 2021 (1st prize)
3. HuNDoC 2020 – 4th Hungarian Neuroscience Meeting for Undergraduate Students, Graduate Students and Junior Postdocs, Szeged, Hungary
4. 16th Congress of Hungarian Neuroscience Society, 2019, Debrecen, Hungary
5. HuNDoC 2019 - 3rd Hungarian Neuroscience Meeting for Undergraduate Students, Graduate Students and Junior Postdocs, Debrecen, Hungary
6. XXI. Scientific Forum of Korányi Frigyes 2018, Budapest, Hungary (2nd prize)
7. Annual Scientific Students' Conference 2018, Semmelweis University, Budapest, Hungary
8. Annual congress of the Hungarian Medical Association of America in Balatonfüred, 2017 (1st prize in the section, and Iván Krisztinicz Award for the best English presentation of the conference)
9. 20th Congress of the Hungarian Anatomical Society, 2017
10. Annual Scientific Students' Conference 2017, Semmelweis University, Budapest, Hungary (1st prize)
11. National Scientific Students' Conference 2017, Pécs
12. The 24th Students' Scientific Conference 2017, Târgu Mureș, Romania
13. XXI. Scientific Forum of Korányi Frigyes 2016, Budapest, Hungary
14. Annual Scientific Students' Conference 2016, Semmelweis University, Budapest, Hungary

DOI:10.14753/SE.2023.2813

11. Acknowledgements

I would like to express my special thanks of gratitude to my supervisor, Prof. Árpád Dobolyi, for the patient guidance, encouragement and advice he has provided throughout my time as his student. I have been extremely fortunate to have a supervisor who cared so much about my work and personal development, and who responded to my questions and queries so promptly. I am pleased that I could learn how to be a good researcher from him.

I would like to also extend my gratitude to all the members of the Laboratory of Neuromorphology, whose continuous support helped me through my doctoral years. I am grateful to Melinda Vitéz-Cservenák, with whom I started my first research project, to Éva Renner for her daily soul-stirring advice, Fanni Dóra to be my associate during the doctoral years and Tamás Láng and Luca Darai for their assistance with my projects. This thesis would have been not possible without the technical support of Viktória Dellaszéga-Lábas, Nikolett Hanák and Erzsébet Horváthné Oszwald. I am thankful for their thorough work and I am feeling lucky that I was able to learn the technical skills from them. I also appreciate the guidance of Magdolna Toronyay-Kasztner, especially in scientometrics. I cannot thank enough Szilvia Deák and Zoltán Gróti for their assistance with the animals. Altogether, I am delighted for working together with these people and for sharing so many memories.

I would also like to thank András Lékó, Gina Puska and János Barna for their advice and help during my doctoral years. I am also grateful for Vivien Csikós, Szilvia Oláh and Diána Dimén for their support and for our stimulating conversations which guided me through difficult times. I would like to also thank Prof. Miklós Palkovits for all his insights into my project and advice on my personal development. I also appreciate our collaborators from the University of Heidelberg, especially Prof. Valery Grinevich. I am obliged to Prof. Alán Alpár and all members of the Department of Anatomy, Histology and Embryology for their help.

I would also like to give special thanks to my family and my friends as a whole for their continuous support and understanding my devotion to my research and to writing my project.

DOI:10.14753/SE.2023.2813

Funding

Support was provided by Hungarian National Research, Development and Innovation Office OTKA K134221, NKFIH-4300-1/2017-NKP_17-00002, the National Brain Research Program 3 (NAP3) of the Hungarian Academy of Sciences, and the Excellence Program of the Semmelweis University for AD; Gedeon Richter Plc. Centenary Foundation (Gyömrői út 19-21. Budapest, 1103), New National Excellence Program of the Ministry of Innovation and Technology and Doctoral Student Scholarship Program of the Co-operative Doctoral Program of the Ministry of Innovation and Technology financed from the National Research and EFOP-3.6.3-VEKOP-16-2017-00009 for DK.

DOI:10.14753/SE.2023.2813

NYILATKOZAT EREDETISÉGRŐL ÉS SZERZŐI JOGRÓL

a PhD disszertáció elkészítésére vonatkozó szabályok betartásáról

Alulírott, Dr. Keller Dávid jelen nyilatkozat aláírásával kijelentem, hogy a POSTERIOR INTRALMINAR COMPLEX OF THE THALAMUS AFFECTS SOCIAL INTERACTIONS című PhD értekezésem önálló munkám, a dolgozat készítése során betartottam a szerzői jogról szóló 1999. évi LXXVI tv. vonatkozó rendelkezéseit, a már megjelent vagy közlés alatt álló közlemény(ek)ből felhasznált ábra/szöveg nem sérti a kiadó vagy más jogi vagy természetes személy jogait.

Jelen nyilatkozat aláírásával tudomásul veszem, hogy amennyiben igazolható, hogy a dolgozatban nem saját eredményeimet használtam fel vagy a dolgozattal kapcsolatban szerzői jog megsértése merül fel, a Semmelweis Egyetem megtagadja PhD dolgozatom befogadását, velem szemben fegyelmi eljárást indít, illetve visszavonja a már odaítélt PhD fokozatot.

A dolgozat befogadásának megtagadása és a fegyelmi eljárás indítása nem érinti a szerzői jogsértés miatti egyéb (polgári jogi, szabálysértési jogi, büntetőjogi) jogkövetkezményeket.

Tudomásul veszem, hogy a PhD értekezés nyilvánosan elérhető formában feltöltésre kerül az Országos Doktori Tanács honlapjára.

Budapest, 2022. 09. 22.

aláírás